Supporting Information for

Ion Specific Fluorescence Modulation of Polyvinyl Alcohol-Boronate Matrices

Brian P. Jacobs, Jacob Townsend, Konstantinos D. Vogiatzis, and Johnathan N. Brantley

Department of Chemistry, University of Tennessee, Knoxville, Tennessee 37916

Email: jbrant13@utk.edu

Table of Contents

1 General Considerations

1.1 Materials and Methods

All solvents and reagents were obtained from commercial sources and used without further purification, and none of the chemical manipulations required exclusion of oxygen or water. ^{1}H, ^{11}B, ^{13}C, and ^{19}F NMR data were collected on a Varian 300 MHz NMR, a Bruker 400 MHz NMR, or a Varian 500 MHz NMR spectrometer. Chemical shifts (δ) for spectra are reported in ppm using the residual solvent as reference (^{1}H and ^{13}C), no references (^{11}B and ^{19}F), or using benzotrifluoride as an internal standard for noted ^{19}F spectra. UV-visible absorbance spectra were recorded using an Agilent Cary 100 series UV-vis spectrophotometer and quartz cuvettes. Fluorescence emission spectra were recorded using an Agilent Cary Eclipse Fluorescence Spectrophotometer. Thermogravimetric analysis (TGA) was performed on a TA Instruments TGA Q500 and Dynamic Mechanical Analysis (DMA) data was collected on a TA Instruments DMA Q800 with a film tension clamp. Gel Permeation Chromatography (GPC) data was collected on an Omnisec Resolve and Omnisec Reveal System using triple detection with detectors in series: UV, light scattering, viscometer, and refractive index and three Viscotek styrene divinylbenzene copolymer columns (in series T3000, T4000, and T5000) at a flow rate of 1 mL/min and thermostatted to 30 °C using tetrahydrofuran (THF) as the eluent. Absolute molecular weight and dispersity data are reported.

2 Synthetic Considerations

2.1 Syntheses of 4_R

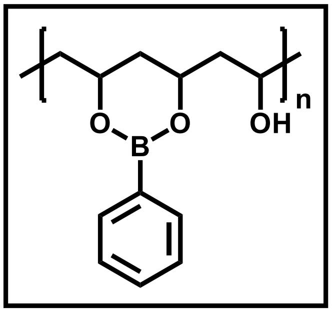

The polymer $\mathbf{4_H}$ was prepared in a one-step synthesis. A 100-mL round bottom flask was charged with a Teflon stir bar, polyvinyl alcohol (**PVA**; M_n = 67 kDa; 1.20 g, 27.2 mmol) and dimethyl sulfoxide (DMSO, 40 mL). Upon complete dissolution of the **PVA** solid, phenylboronic acid (**PBA**; 1.66 g, 13.6 mmol) and 4 Å molecular sieves (5 g) were added to the DMSO mixture. The round bottom flask was sealed with a rubber septum, and the reaction mixture was heated to 150 °C with stirring over 3 h. After the mixture was cooled to 23 °C, the mixture was filtered, and the filter cake was washed with DMSO (10 mL). The combined DMSO solutions were added dropwise to a stirring solution of methanol (MeOH, 150 mL), resulting in immediate precipitation of a colorless solid. The solid was collected *via* vacuum filtration and washed with MeOH (50 mL). The crude solid was dissolved in chloroform ($CHCl_3$, 20 mL), and the $CHCl_3$ solution was added dropwise to MeOH (100 mL) to precipitate $\mathbf{4_H}$ as a colorless solid (1.178 g, 59% yield), which was collected *via* vacuum filtration. NMR spectra for the precipitated material were collected in $CDCl_3$ (Figures S21-S23). ^{1}H NMR ($CDCl_3$): δ 1.47-2.41 (7H), 3.20-5.72 (3H), 7.28-7.52 (3H), 7.83 (2H).` ^{13}C NMR ($CDCl_3$): δ 39.65, 45.08, 65.43, 68.67, 127.71, 130.86, 132.82, 133.97. ^{11}B NMR ($CDCl_3$): δ 26.56.

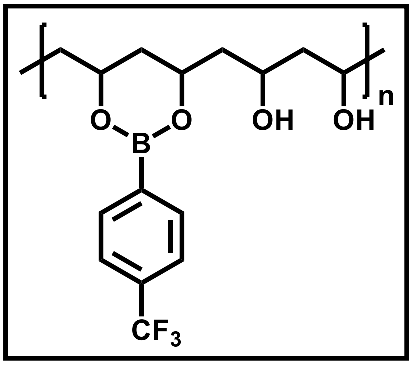

The polymer **4$_{CF3}$** was prepared in a one-step synthesis. A 50-mL round bottom flask was charged with a Teflon stir bar, **PVA** (*M$_n$* = 67 kDa; 500 mg, 11.4 mmol) and DMSO (20 mL). Upon complete dissolution of the **PVA** solid, **PBA**-*p*-CF_3 (1.08 g, 5.70 mmol) and 4 Å molecular sieves (2 g) were added to the DMSO mixture. The round bottom flask was sealed with a rubber septum, and the reaction mixture was heated to 150 °C with stirring over 14 h. The mixture was filtered through a medium fritted disk filter funnel *via* vacuum filtration with the mixture at 150 °C, and the filtered residue was washed with hot DMSO (150 °C, 10 mL). The combined DMSO solutions were heated to 150 °C, and subsequently added dropwise to a stirring solution of methanol (MeOH, 100 mL), resulting in immediate precipitation of a colorless solid. The solid was collected *via* vacuum filtration and washed with MeOH (50 mL). The crude solid was tritrated with MeOH (2 x 50 mL), and isolated *via* filtration to afford **4$_{CF3}$** as a colorless solid (676 mg, 62% yield). **Note**: Allowing the initial DMSO solution to cool to 23 °C prior to removing the molecular sieves *via* filtration results in deposition of **4$_{CF3}$** as a filmy residue that is difficult to collect. NMR spectra for the precipitated material were collected in THF-d$_8$ (Figures 2 and S24). ^{1}H NMR (D_8-THF): δ 1.44-2.39 (8H, corrected with D_8-THF integration (2.76) subtracted from total peak (10.76)), 3.69-5.55 (4H), 7.59 (2H), 7.96 (2H). ^{13}C NMR (D_8-THF): δ 40.42, 46.24, 69.68, 124.91, 125.63 (q, 274 Hz, CF_3), 132.80, 135.21, 138.80. ^{11}B NMR (D_8-THF): δ 27.64. ^{19}F NMR (D_8-THF): δ -63.13.

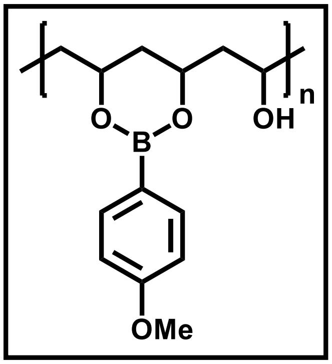

The polymer **4$_{OMe}$** was prepared in a one-step synthesis. A 50-mL round bottom flask was charged with a Teflon stir bar, **PVA** (*M$_n$* = 67 kDa; 500 mg, 11.4 mmol), and DMSO (20 mL). Upon complete dissolution of the **PVA** solid, **PBA**-*p*-OMe (862 mg, 5.70 mmol) and 4 Å molecular sieves (2 g) were added to the DMSO mixture. The round bottom flask was sealed with a rubber septum, and the reaction mixture was heated to 150 °C with stirring over 14 h. After the mixture was cooled to 23 °C, the mixture was filtered, and the filtered residue was washed with DMSO (10 mL). The combined DMSO solutions were added dropwise to a stirring solution of methanol (MeOH, 100 mL), resulting in immediate precipitation of a colorless solid. The solid was collected *via* vacuum filtration and washed with MeOH (50 mL). The crude solid was re-precipitated three times by dissolving it in dichloromethane (CH_2Cl_2, 5 mL) and adding this solution to MeOH (50 mL). **4$_{OMe}$** was collected as a colorless solid (563 mg, 60% yield) *via* vacuum filtration. NMR spectra for the precipitated material were collected in $CDCl_3$ (Figures S25-S27). ^{1}H NMR ($CDCl_3$): δ 1.45-2.40 (7H), 3.80 (3H), 3.89-5.71 (3H), 6.87 (2H), 7.77 (2H). ^{13}C NMR ($CDCl_3$): δ 39.04, 44.13, 55.19, 65.21, 68.60, 113.28, 124.61, 135.28, 161.88. ^{11}B NMR ($CDCl_3$): δ 26.06.

3 Material Characterization

3.1 UV-vis and Fluorescence Characterization

Initial fluorescence observations of **4$_R$** matrices (in both solid state and solution) were facilitated by a Model UVL-21 Blak-Ray Lamp from UVP, Inc. (employing long wave UV-366nm; Figure S1). All other quantitative measurements for both UV-vis and fluorescence were conducted using the instrumentation noted in the General Considerations section. All measurements were recorded using either N,N-dimethylformamide (DMF) or DMSO as solvent (noted in specific figure captions). Samples that were used for collecting UV-vis spectra were immediately used to acquire fluorescence spectra.

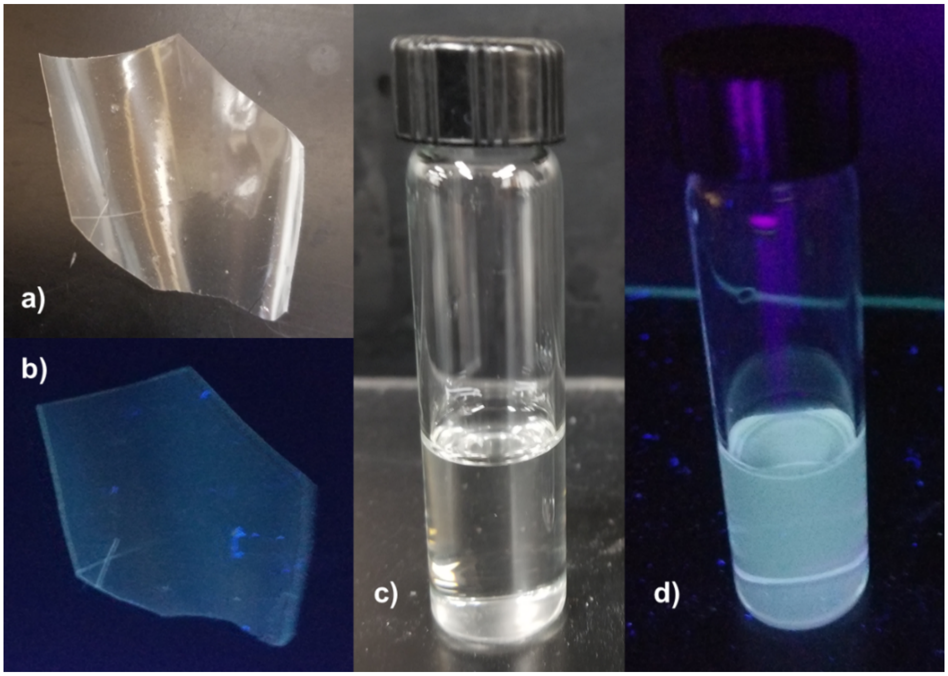

Figure S1: Solid film of **4**$_\text{H}$ Under Ambient Light (a) and Under a 366 nm UV Lamp (b). DMF Solution of **4**$_\text{H}$ Under Ambient Light (c) and Under a 366 nm UV Lamp (d)

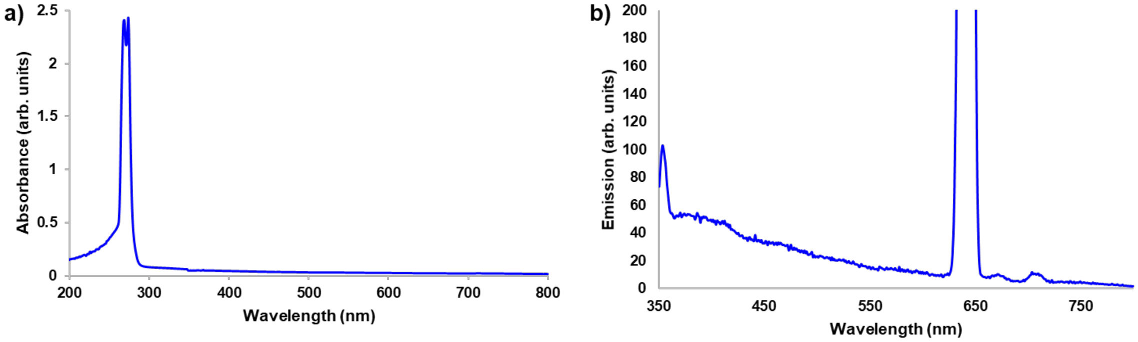

Figure S2: UV-vis Absorbance (a) and Fluorescence (b) Spectra of **4**$_\text{H}$ in DMF (7 mM)

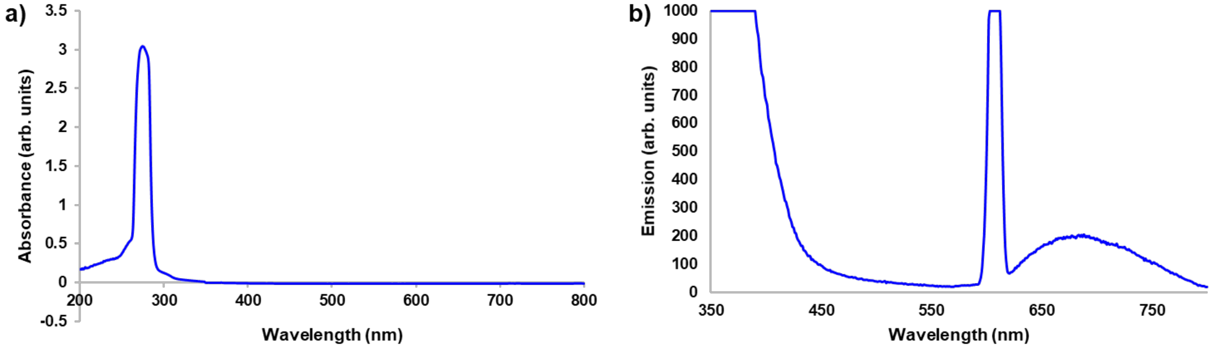

Figure S3: UV-vis Absorbance (a) and Fluorescence (b) Spectra of **4**$_\text{OMe}$ in DMF (7 mM)

3.2 GPC Traces and Thermomechanical Data

GPC data for the isolated polymers are presented in Figure S4. Representative thermomechanical data of the isolated **4**$_R$ materials are presented in Figures S5, S6, and S7. The TGA thermograms of powdered samples of each **4**$_R$ material are presented in Figure S5. Polymers **4**$_H$ and **4**$_{OMe}$ bear negligible mass losses prior to 300 ^oC, originating from residual water and DMSO solvents. Each polymer exhibits three similar decomposition onset points: **4**$_H$ (316, 374, and 421 ^oC); **4**$_{CF3}$ (293, 347, and 412 ^oC); **4**$_{OMe}$ (307, 365, and 423 ^oC). Rectangular films of each polymer were cast from THF (10 weight percent polymer) and analyzed using DMA (with a tension fiber clamp). The stress frequency sweep plots are provided in Figure S6. No transitions were observed under 23 ^oC for any of the tested polymers. Temperature values at Tan δ_{MAX} are as follow: **4**$_H$ (140 ^oC); **4**$_{CF3}$ (125 ^oC); **4**$_{OMe}$ (145 ^oC). Traces for **4**$_H$ and **4**$_{OMe}$ ended once the rectangular film samples yielded. The stress strain plots are given in Figure S7, and both Young's modulus and strain at break are presented for each material: **4**$_H$ (~2.2 GPa, 6.28%); **4**$_{CF3}$ (~3.9 GPa, 1.51%); **4**$_{OMe}$ (~3.3 GPa, 13.08%).

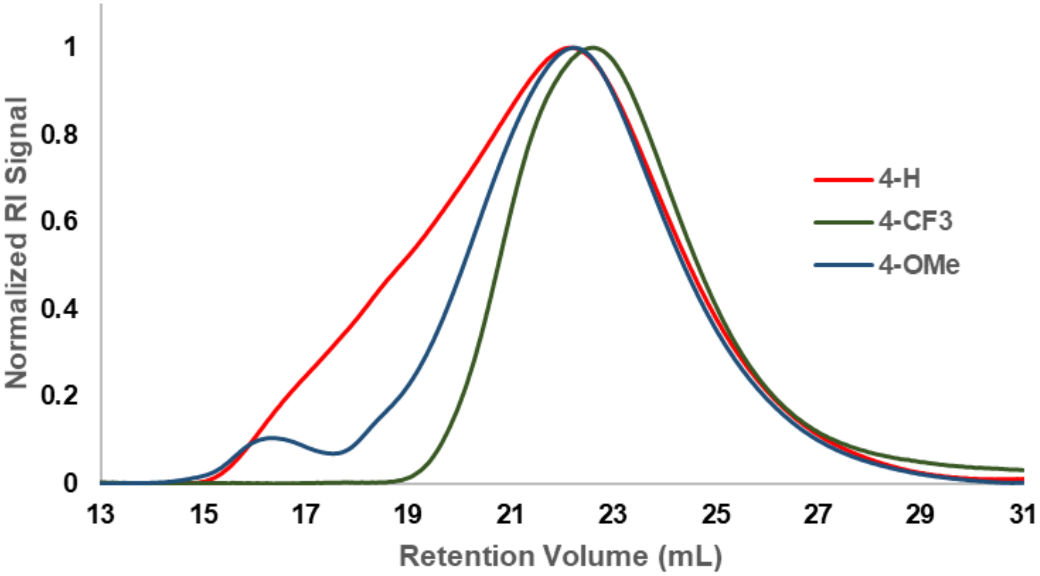

Figure S4: GPC Traces of Isolated **4**$_R$ Materials. Calculated molecular weights are as follows: M_n (**4**$_H$) = 64,260 Da; M_n (**4**$_{CF3}$) = 94,770 Da; M_n (**4**$_{OMe}$) = 63,660 and 308,500 Da.

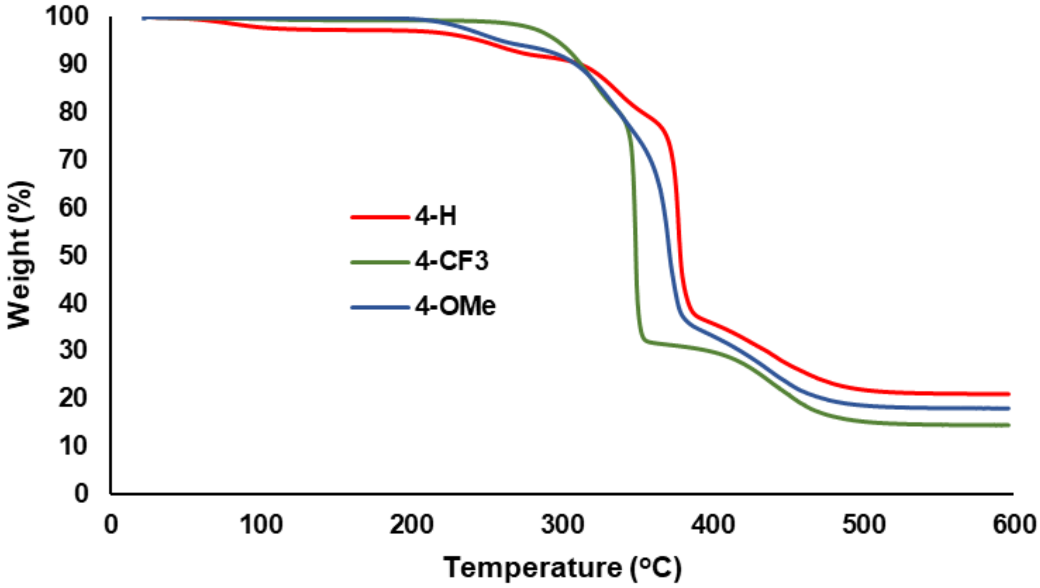

Figure S5: Representative TGA Thermograms of Isolated **4**$_{\mathbf{R}}$ Materials (10 ºC min^{-1})

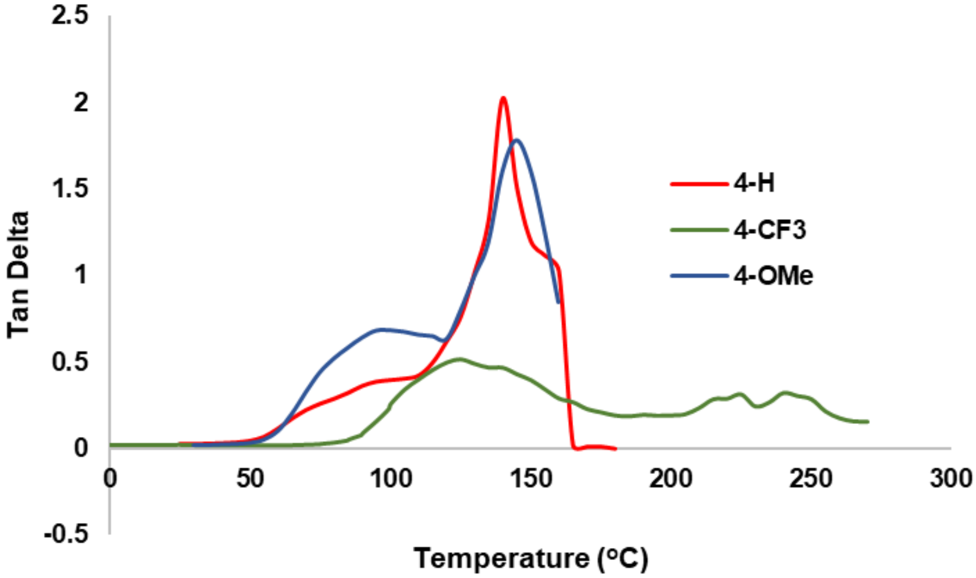

Figure S6: Representative DMA Stress Frequency (5 Hz) Sweep Plots of Isolated **4**$_{\mathbf{R}}$ Materials

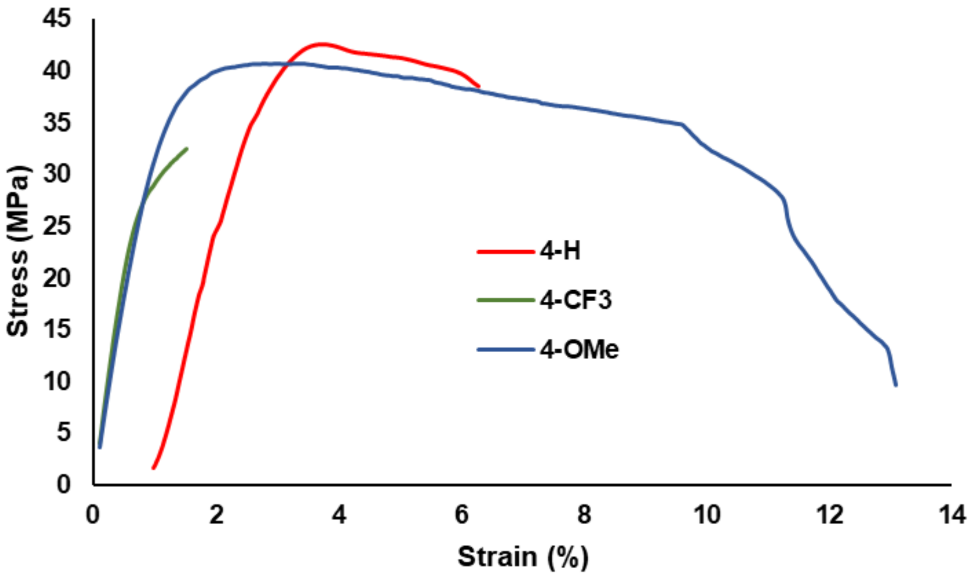

Figure S7: Representative DMA Stress Strain Plots of Isolated $\mathbf{4_R}$ Materials

4 Anion Addition Experiments

4.1 Stoichiometric Hydroxide Addition to $\mathbf{4_R}$

4.1.1 Stoichiometric Hydroxide Addition to $\mathbf{4_H}$

A 2-dram vial was charged with $\mathbf{4_H}$ (15 mg, 67 μmol) and DMSO-d_6 (0.5 mL). A ^{1}H NMR spectrum was acquired of the solution, followed by addition of TBAOH (0.27 mL of a 1 M solution in MeOH, 0.27 mmol). Subsequent ^{1}H NMR analysis of the mixture indicated an upfield shift of the aromatic resonances. Sharp resonances were observed in the spectrum (6.86, 7.00, and 7.38 ppm), along with a new broad resonance at 4.01 ppm. These data were consistent with modest decomposition of $\mathbf{4_H}$ (the percent decomposition could not be determined since the new aromatic resonances were isochronous with those of the product polymer). The spectra are provided in Figure S28.

4.1.2 Stoichiometric Hydroxide Addition to Phenylboronic Acid (**PBA)**

A 2-dram vial was charged with **PBA** (12 mg, 0.1 mmol), TBAOH (0.2 mL of a 1 M solution in MeOH, 0.2 mmol), and DMSO-d_6 (0.5 mL). Subsequent ^{1}H NMR analysis of the resultant solution revealed new aromatic resonances at 6.85 (1H, t, 7 Hz), 6.99 2H, t, 7 Hz), and 7.37 (2H, d, 7 Hz) ppm, consistent with quantitative formation of a boronate complex. The spectrum is provided in Figure S29, and is overlaid with the spectrum obtained from addition of TBAOH with $\mathbf{4_H}$ (Section 4.1.1). The boronate resonances are consistent with the previously observed decomposition products from Section 4.1.1, (which suggests cleavage of the boronic esters within $\mathbf{4_H}$ to afford discreet, small molecule boronates).

4.1.3 Stoichiometric Hydroxide Addition to $\mathbf{4_{CF3}}$

A 2-dram vial was charged with $\mathbf{4_{CF3}}$ (12 mg, 36 μmol) and DMSO-d_6 (0.5 mL). The solution was analyzed by ^{19}F NMR spectroscopy, and TBAOH (0.17 mL of a 1 M solution in MeOH, 0.17 mmol) was subsequently added. The mixture was analyzed by ^{19}F NMR spectroscopy, which indicated a downfield shift of the aryl-CF_3 resonance from -61.74 to

-60.65 ppm. The growth of a sharp resonance at -60.57 ppm was taken to indicate modest decomposition of the polymer (percent decomposition could not be determined since the sharp singlet was not resolved from the resonance attributed to the polymer). The spectrum is provided in Figure S30.

4.2 Anion Titration Experiments of **4**$_{\text{CF3}}$

4.2.1 Hydroxide Addition Methodology

A 2-dram vial was charged with **4**$_{\text{CF3}}$ (10 mg, 30 µmol) and DMF (5 mL). UV-vis absorbance and fluorescence spectra (λ_{EX} = 320 nm) were recorded. TBAOH (0.04 mL from a 1 M MeOH solution, 35 µmol) was added to the polymer solution, and both UV-vis absorbance and fluorescence spectra were recorded. This method was repeated for five additional cycles (for a total of 7 equivalents of hydroxide). The spectra are presented in Figure 2.

4.2.2 Other Anion Addition Methodology

A 2-dram vial was charged with **4**$_{\text{CF3}}$ (10 mg, 30 µmol) and DMF (5 mL). UV-vis absorbance and fluorescence spectra (λ_{EX} = 320 nm) were recorded. A solid sample of a given anion (35 µmol of the tetrabutylammonium salt) was added to the polymer solution, and both UV-vis absorbance and fluorescence spectra were recorded. This method was repeated for five additional cycles (for a total of 7 equivalents of the anion). Spectra for the fluoride and cyanide experiments are presented in Figure 2, while the remaining anions of interest are presented in Figures S8-12.

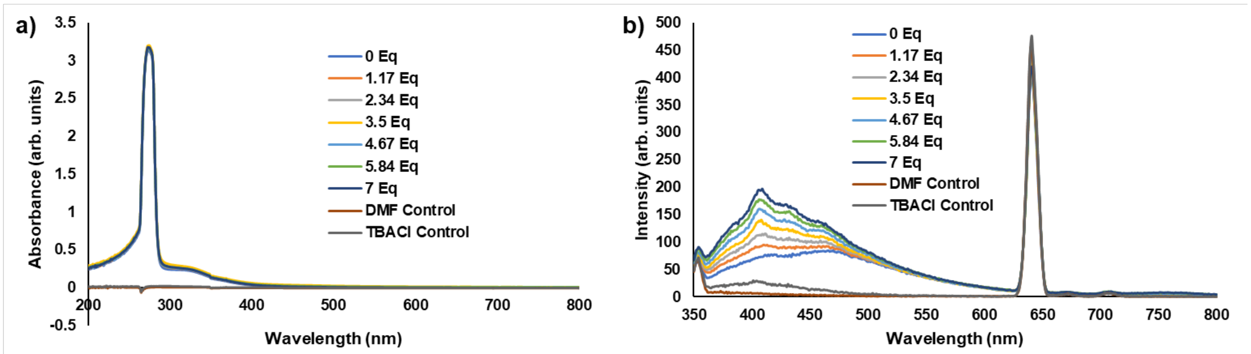

Figure S8: **4**$_{\text{CF3}}$ + Chloride UV-vis Absorbance (a) and Fluorescence (b) Spectra

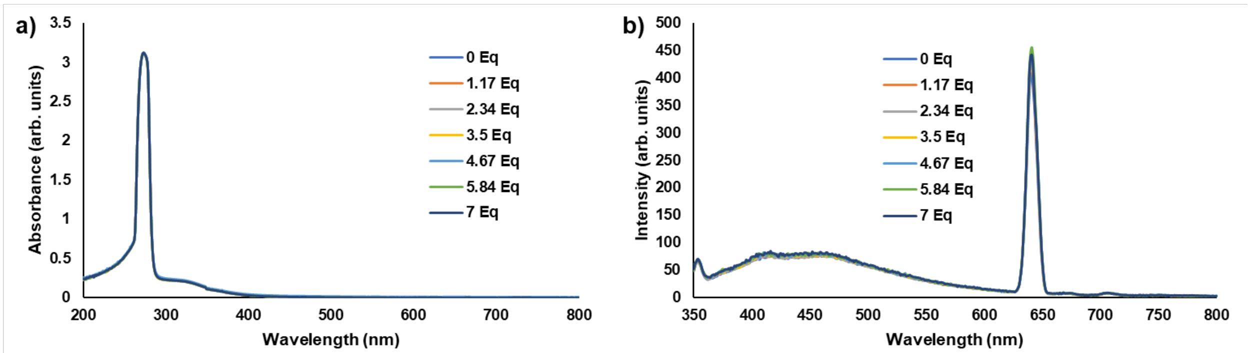

Figure S9: **4**$_{\text{CF3}}$ + Bromide UV-vis Absorbance (a) and Fluorescence (b) Spectra

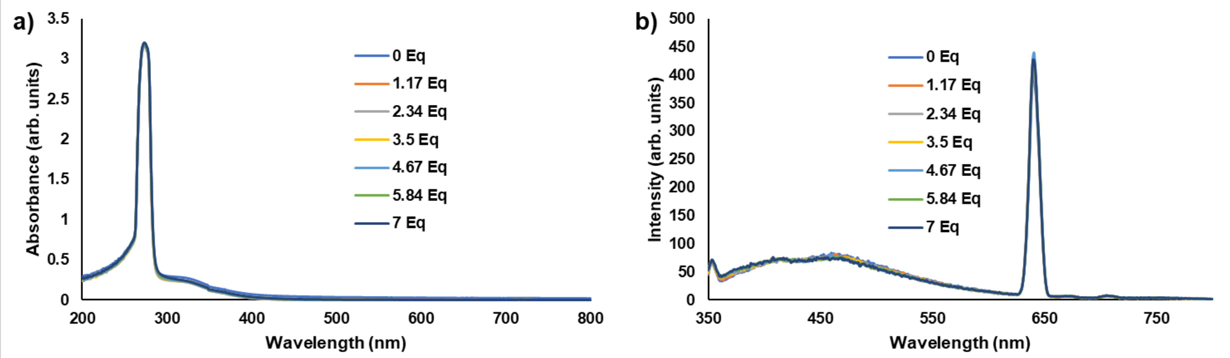

<u>Figure S10:</u> **4_{CF3}** + Iodide UV-vis Absorbance (a) and Fluorescence (b) Spectra

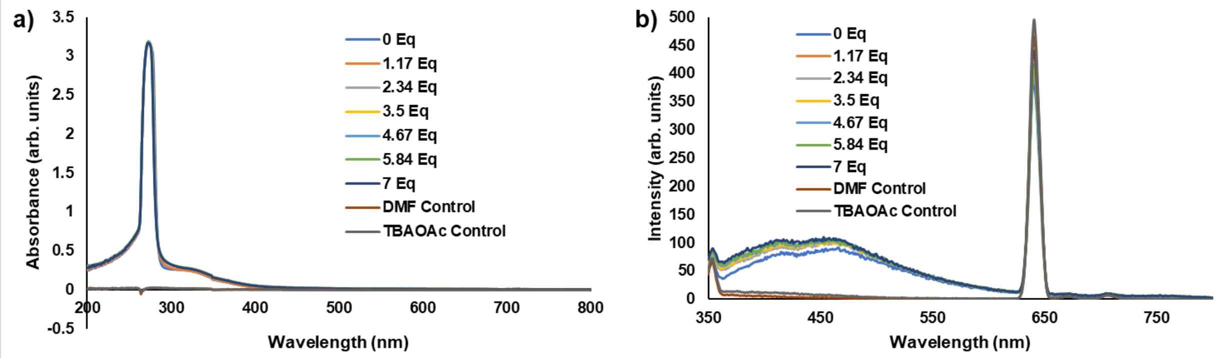

<u>Figure S11:</u> **4_{CF3}** + Acetate UV-vis Absorbance (a) and Fluorescence (b) Spectra

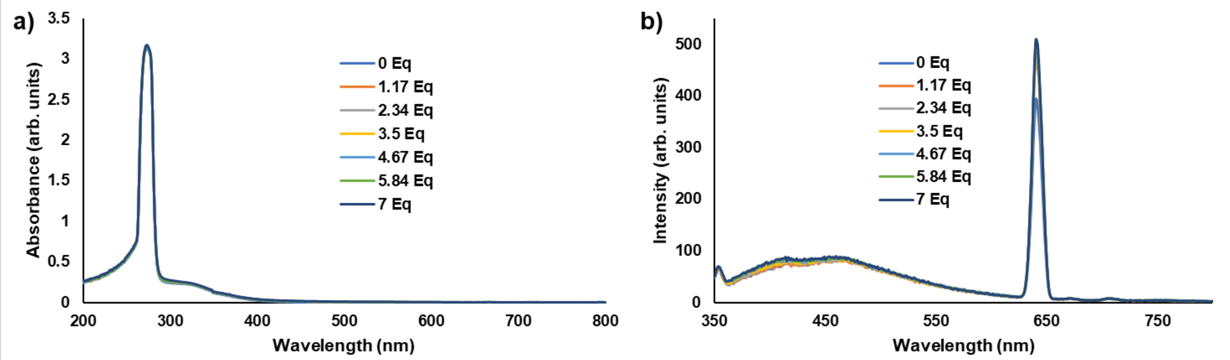

<u>Figure S12:</u> **4_{CF3}** + Hydrogen Sulfate UV-vis Absorbance (a) and Fluorescence (b) Spectra

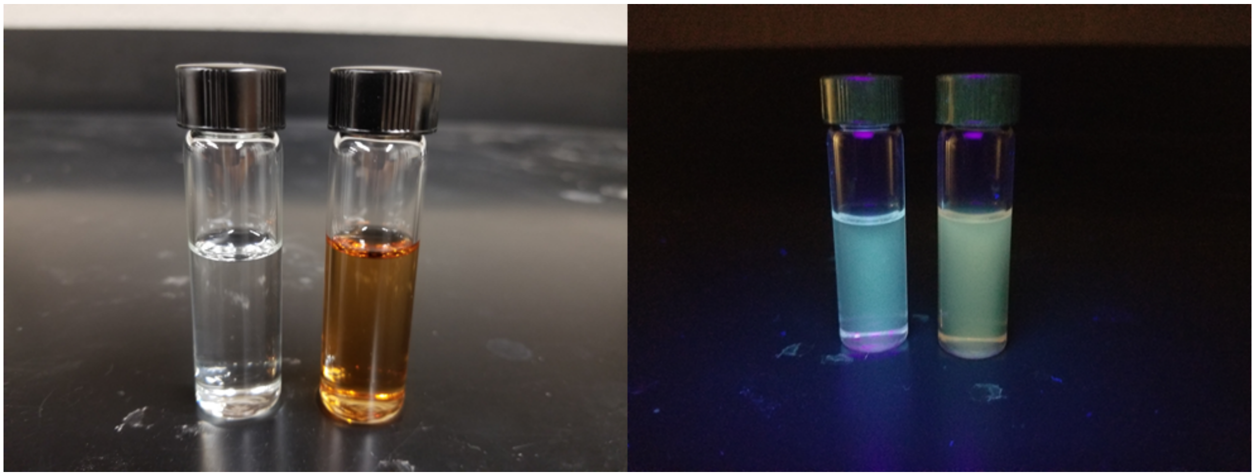

Figure S13: Solution of $\mathbf{4_{CF3}}$ in DMF Under Visible (Left Image) or UV (Right Image) Light with (Right Vial) or without (Left Vial) TBAF

4.3 Anion Titration Experiments of PVA

A 2-dram vial was charged with **PVA** (2.0 mg, 45 µmol) and DMSO (5 mL). UV-vis absorbance and fluorescence spectra were acquired (λ_{EX} = 320 nm) for the **PVA** mixture, and $TBAF \cdot 3H_2O$ (14 mg, 45 µmol) was subsequently added. The UV-vis absorbance and fluorescence spectra for the mixture were recorded, and they are provided in Figure S14.

Identical procedures were replicated for the following experiments: (1) **PVA** (2.6 mg, 59 µmol) with TBAOH (0.06 mL from a 1 M MeOH solution, 59 µL), and (2) **PVA** (2.8 mg, 64 µmol) with TBACN (17 mg, 64 µmol). Results are provided in Figure S14.

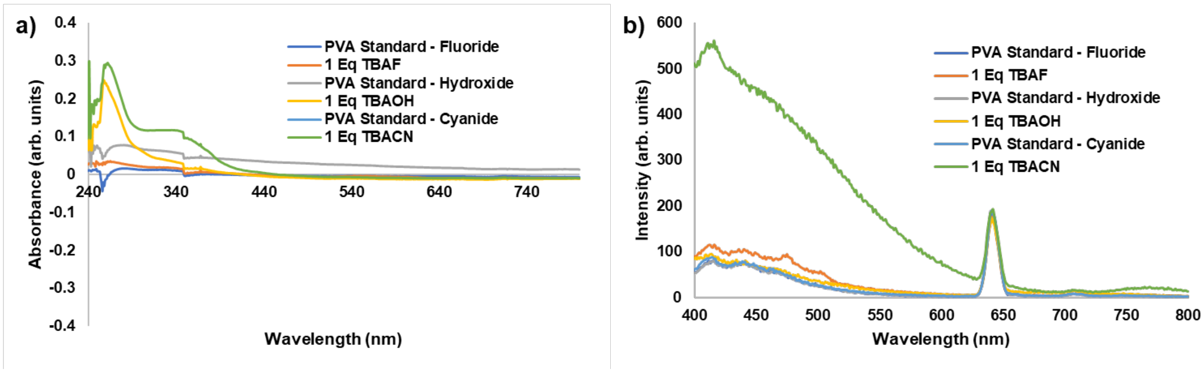

Figure S14: UV-vis Absorbance (a) and Fluorescence (b) Spectra for Anion Additions to **PVA** Solution

4.4 Duplication of Select Anion Titration of $\mathbf{4_{CF3}}$

A 2-dram vial was charged with $\mathbf{4_{CF3}}$ (10 mg, 30 µmol) and DMF (5 mL). UV-vis absorbance and fluorescence spectra (λ_{EX} = 320 nm) were recorded, and TBAF (11 mg, 35 μmol) was added to the polymer solution. UV-vis absorbance and fluorescence spectra were recorded for the resulting solution. This method was repeated for five additional cycles (7 total equivalents of fluoride added). The duplication spectra are presented in Figures S15. Figure S18 compares the normalized intensities ($I_n - I_0$) of these duplication experiments with the original experiments from section 4.2.

Identical procedures were replicated for the following experiments: (1) **4**$_{\mathrm{CF3}}$ (10 mg, 30 μmol) with TBAOH (0.04 mL from a 1 M MeOH solution, 35 μL), and (2) **4**$_{\mathrm{CF3}}$ (10 mg, 30 μmol) with TBACN (9.4 mg, 35 μmol). Results are provided in Figures S16 and S17.

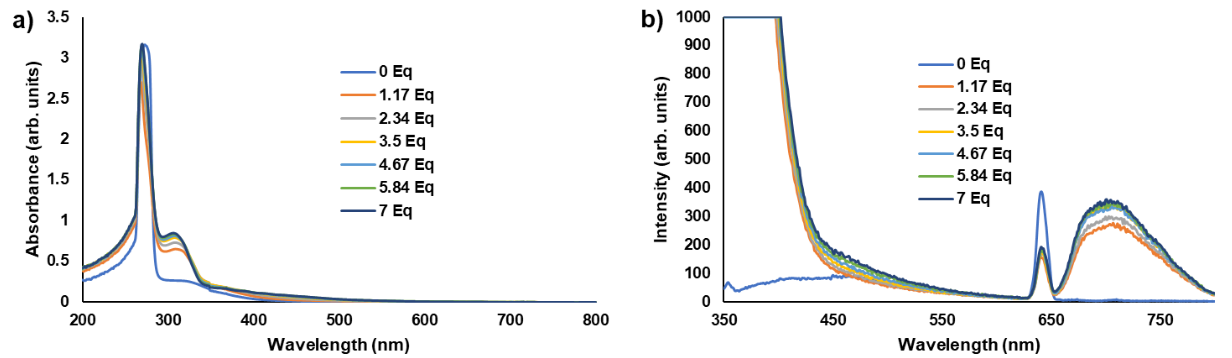

Figure S15: **4**$_{\mathrm{CF3}}$ + Fluoride UV-vis absorbance (a) and Fluorescence (b) Spectra

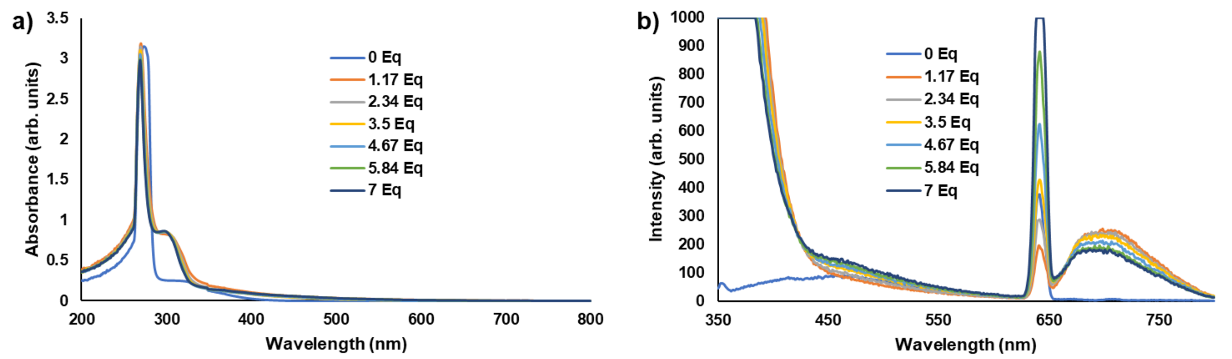

Figure S16: **4**$_{\mathrm{CF3}}$ + Hydroxide UV-vis Absorbance (a) and Fluorescence (b) Spectra

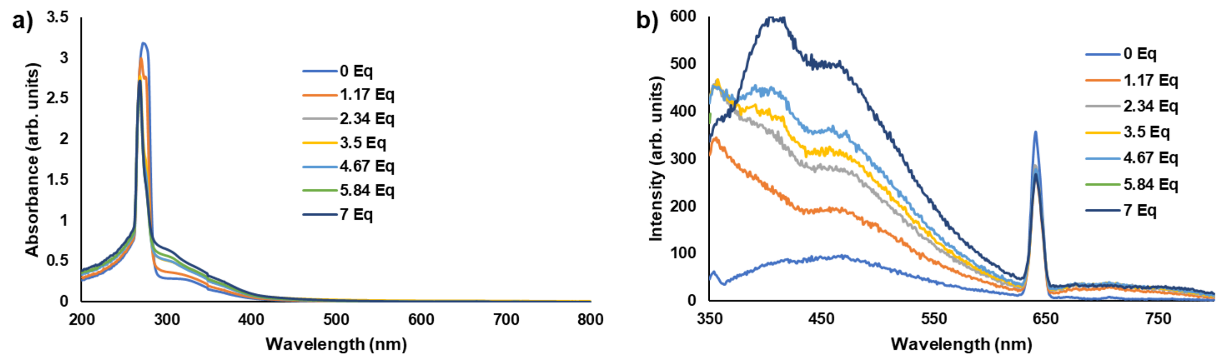

Figure S17: **4**$_{\mathrm{CF3}}$ + Cyanide UV-vis Absorbance (a) and Fluorescence (b) Spectra

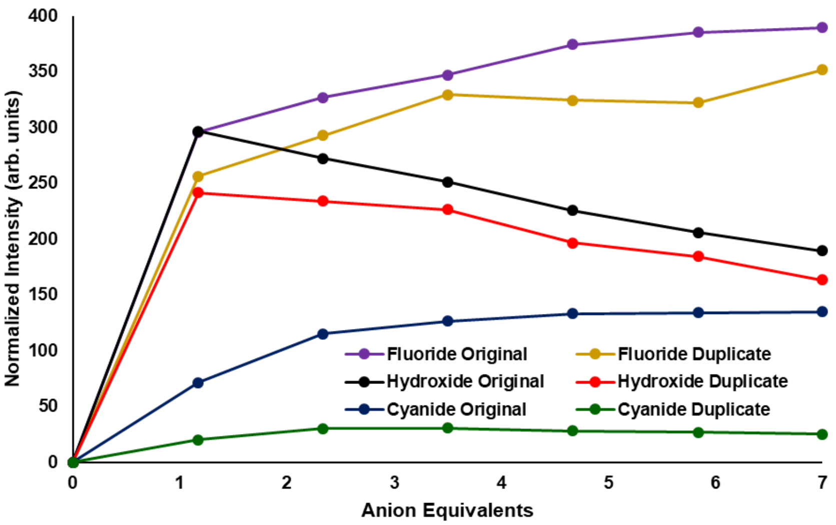

Figure S18: Normalized Fluorescence Comparison Between Original and Duplication Anion Titration Experiments of **4**$_{\mathrm{CF3}}$

4.5 Fluoride Titration Experiments of **4**$_{\mathrm{H}}$ and **4**$_{\mathrm{OMe}}$

A 2-dram vial was charged with **4**$_{\mathrm{H}}$ (7.6 mg, 35 µmol) and DMF (5 mL). UV-vis absorbance and fluorescence spectra (λ_{EX} = 320 nm) were recorded, and $TBAF\cdot 3H_2O$ (11 mg, 35 µmol) was added to the polymer solution. UV-vis absorbance and fluorescence spectra were recorded for the resulting solution. This method was repeated for five additional cycles (6 total equivalents of fluoride added); the spectra are reported in Figure S19.

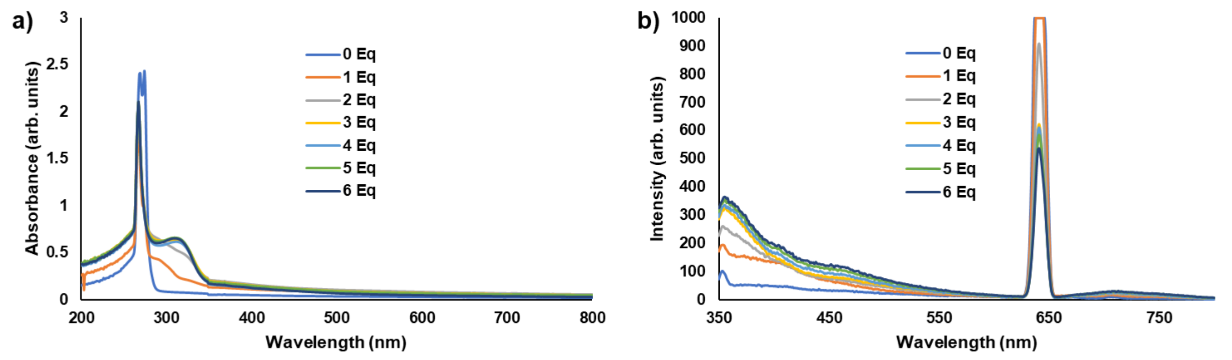

Figure S19: **4**$_{\mathrm{H}}$ + Fluoride UV-vis Absorbance (a) and Fluorescence (b) Spectra

A 2-dram vial was charged with **4**$_{\mathrm{OMe}}$ (8.7 mg, 35 µmol) and DMF (5 mL). UV-vis absorbance and fluorescence spectra (λ_{EX} = 303 nm) were recorded, and $TBAF\cdot 3H_2O$ (11 mg, 35 µmol) was added to the polymer solution. UV-vis absorbance and fluorescence spectra were recorded for the resulting solution. This method was repeated for five additional cycles (6 total equivalents of fluoride added); the spectra are reported in Figure S20.

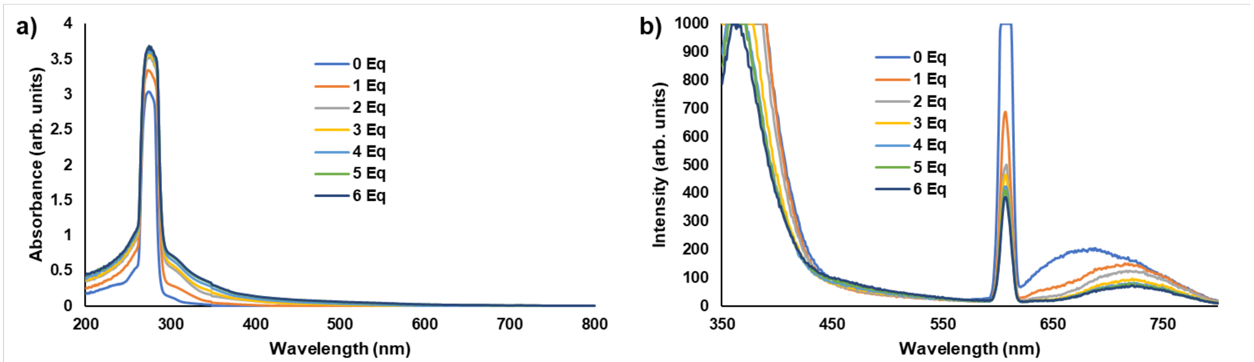

Figure S20: $\mathbf{4_{OMe}}$ + Fluoride UV-vis absorbance (a) and Fluorescence (b) Spectra

5 Fluoride Extraction Experiments

5.1 General Methodology for Fluoride Extraction

A 20-mL scintillation vial was charged with MeOH (9.1 mL), TBAF (1.0 M in THF, 1.35 mmol, 1.35 mL), and benzotrifluoride (0.45 mmol, 55 µL) as the internal standard. The mixture was stirred for 5 min at 23 °C, and subsequently divided up into three equal volume portions in separate 2-dram vials for conducting triplicate experiments (3.5 mL per reaction, 0.15 mmol benzotrifluoride, 0.45 mmol TBAF). Rectangular film samples (cast from 10 w% THF solutions) of the $\mathbf{4_R}$ materials (0.05 mmol) were prepared. A 0.1 mL aliquot from each methanol mixture was removed and set aside to determine initial fluoride equivalents. The polymer film was then submerged in the methanol mixture, and allowed to stand for 24 h at 23 °C. Aliquots (0.1 mL) were taken from the mixture after 1, 2, 4, 8, and 24 h. Each aliquot was diluted with MeOH (0.5 mL), and analyzed using ^{19}F NMR spectroscopy.

Fluoride equivalents were determined from ^{19}F NMR spectra by setting the benzotrifluoride peak integration to nine (consistent with three equivalents of the internal standard), and recording the resultant integration for the TBAF resonance. The fluoride equivalents are noted in Table S1 for all tested materials, including each time point and each run. Plotted time points are the average fluoride integration for each time point, and standard deviations for each time point were used to construct the error bars in Figure 5.

As a control experiment, a **PVA** film (cast from a 5 w% H_2O solution) was used in place of the $\mathbf{4_R}$ materials in the above general methodology. Apart from employing a larger amount of **PVA** (0.1 mmol), the general method was followed as detailed above (Table S1).

As an additional control, $\mathbf{4_{CF3}}$ was tested using potassium fluoride (0.45 mmol per experiment) *in lieu* of TBAF exactly as written in the general method (Table S1).

Table S1: Fluoride Equivalents Extracted Over Time

	Time (h)	0	1	2	4	8	24
$\mathbf{4_{H}}$ + TBAF	*Run 1*	10.15	9.14	9.00	7.56	7.79	6.28
	Run 2	9.39	9.61	9.44	8.08	7.19	6.59
	Run 3	9.83	9.55	9.26	8.64	7.14	6.93
	Average	9.79	9.43	9.23	8.09	7.37	6.60
	St. Dev.	0.382	0.256	0.221	0.540	0.362	0.325
$\mathbf{4_{CF3}}$ + TBAF	*Run 1*	9.30	10.13	9.26	8.50	7.19	6.86
	Run 2	9.29	8.93	7.91	7.71	6.74	6.23
	Run 3	10.2	9.77	9.81	8.37	6.96	7.18
	Average	9.60	9.61	8.99	8.19	6.96	6.76
	St. Dev.	0.523	0.616	0.978	0.424	0.225	0.483
$\mathbf{4_{OMe}}$ + TBAF	*Run 1*	9.86	9.59	8.75	9.72	9.87	9.47
	Run 2	10.41	9.96	9.97	9.54	9.60	9.36
	Run 3	9.81	10.1	10.34	9.96	9.71	9.88
	Average	10.03	9.88	9.69	9.74	9.73	9.57
	St. Dev.	0.333	0.264	0.832	0.211	0.136	0.274
$\mathbf{4_{CF3}}$ + KF	*Run 1*	9.73	9.66	8.70	8.34	7.69	7.47
	Run 2	9.73	8.93	8.24	7.54	7.77	7.12
	Run 3	9.91	9.41	8.70	8.47	7.57	7.66
	Average	9.79	9.33	8.55	8.12	7.68	7.42
	St. Dev.	0.104	0.371	0.266	0.504	0.101	0.274
PVA + TBAF	*Run 1*	6.48	6.52	6.58	6.56	6.72	6.66
	Run 2	6.94	6.74	6.58	6.74	6.77	6.49
	Run 3	6.37	6.44	6.67	6.71	6.91	6.52
	Average	6.60	6.57	6.61	6.67	6.80	6.56
	St. Dev.	0.302	0.155	0.052	0.096	0.098	0.091

5.2 Recyclability Test for Fluoride Extraction with $\mathbf{4_{CF3}}$

A 2-dram vial was charged with MeOH (3 mL), TBAF$\cdot$3H$_2$O (104 mg, 0.33 mmol), and benzotrifluoride as an internal standard (13.5 µL, 0.11 mmol). A 0.1 mL aliquot of the mixture was removed and set aside to determine the initial fluoride equivalents for the first extraction (Figure S31). A rectangular film (cast from 10 w% THF solutions) of $\mathbf{4_{CF3}}$ materials (0.05 mmol) was prepared, and subsequently submerged in the methanolic solution for 24 h at 23 ^{o}C. An additional 0.1 mL aliquot was removed from the solution for determination of the fluoride equivalents after the extraction. The solution was decanted, and the polymer film was washed with DI H$_2$O (3 x 5 mL) and dried under reduced pressure. A second methanol solution of TBAF$\cdot$3H$_2$O and benzotrifluoride was prepared with identical amounts as the first solution. An aliquot of the second methanol mixture was removed and set aside for fluoride equivalent determination, and the film was subsequently submerged in the methanolic solution for 24 h at 23 ^{o}C. A 0.1 mL aliquot was removed from the second methanol mixture. Each aliquot was diluted with MeOH (0.5 mL) and ^{19}F NMR spectra were acquired for each sample to quantify the equivalents of fluoride removed from each methanol solution (employing a single polymer film).

For the first fluoride extraction sequence, t_0 and t_{24} aliquots indicated fluoride equivalents of 9.17 and 7.21, respectively (Figures S31 and S32). For the second extraction sequence, the measured fluoride equivalents were 9.01 and 8.58 (Figures S33 and S34). These results indicate that equivalents of fluoride removed for the first and second extraction sequences were 1.96 and 0.43 equivalents, respectively. DI H_2O recycling of the used $\mathbf{4}_{\mathbf{CF3}}$ film allowed for additional removal of fluoride, albeit only with 22% the efficiency of the first extraction sequence. In addition, ^{11}B NMR of the t_{24} aliquot for the first extraction sequence revealed the presence of small molecule aryl boronate byproducts (Figure S35), indicating that boron leaching does occur from the film materials.

5.3 Homogeneous Fluoride Addition Reactions

5.3.1 Fluoride Addition to $\mathbf{4}_{\mathbf{CF3}}$

A 2-dram vial was charged with either DMF-d_7 or DMSO-d_6 (0.5 mL; ^{19}F NMR spectra acquired in DMF-d_7, ^{11}B NMR spectra acquired in DMSO-d_6), $\mathbf{4}_{\mathbf{CF3}}$ (10 mg, 30 μmol), and TBAF$\cdot$3H_2O (22 mg, 70 μmol). ^{11}B and ^{19}F NMR spectra were then acquired for the reaction mixture. The ^{11}B NMR spectrum revealed a single broad resonance at 2.25 ppm (Figure S36), while the ^{19}F NMR spectrum revealed resonances at -60.68, -60.82, and -137.29 ppm (Figure S37). The peaks at -115.33 and -148.65 ppm are consistent with free TBAF and HF_2^- (the latter assignment consistent with values provided in reference 13). The integration of the B-F -ate complex resonance at -137.29 ppm was 0.26 (relative to 3.00 for the CF_3 group of $\mathbf{4}_{\mathbf{CF3}}$), suggesting reversible -ate complex formation.

5.3.2 Fluoride Addition to $\mathbf{4}_{\mathbf{H}}$

A 2-dram vial was charged with either DMF-d_7 or DMSO-d_6 (0.5 mL; ^{19}F NMR spectra acquired in DMF-d_7, ^{11}B NMR spectra acquired in DMSO-d_6), $\mathbf{4}_{\mathbf{H}}$ (20 mg, 92 μmol), TBAF$\cdot$3H_2O (58 mg, 0.19 mmol), and benzotrifluoride as an internal standard (11.3 μL, 0.092 mmol). ^{11}B and ^{19}F NMR spectra were acquired of the reaction mixture. The ^{11}B NMR spectrum revealed a single broad peak at 4.08 ppm (Figure S38), while the ^{19}F NMR spectrum revealed a broad resonance at –137.63 ppm, consistent with polymer B-F -ate complex formation (Figure S39). The resonances at -117.62 and -150.16 ppm were consistent with free TBAF and HF_2^- (the latter assignment consistent with values provided in reference 13). The integration of the B-F -ate complex is 0.49 (relative to 3.00 for benzotrifluoride), suggesting reversible -ate complex formation.

5.3.3 Fluoride Addition to $\mathbf{4}_{\mathbf{OMe}}$

A 2-dram vial was charged with either DMF-d_7 or DMSO-d_6 (0.5 mL; ^{19}F NMR spectra acquired in DMF-d_7, ^{11}B NMR spectra acquired in DMSO-d_6), $\mathbf{4}_{\mathbf{OMe}}$ (23 mg, 93 μmol), TBAF$\cdot$3H_2O (59 mg, 0.19 mmol), and benzotrifluoride as an internal standard (11.4 μL, 0.099 mmol). ^{11}B and ^{19}F NMR spectra were acquired of the reaction mixture. The ^{11}B NMR spectrum revealed a single broad peak at 4.08 ppm (Figure S40), while the ^{19}F NMR spectrum of the reaction mixture reveal a broad resonance at –136.75 ppm, consistent with polymer B-F -ate complex formation (Figure S41). The peaks at -116.643 and -149.88 ppm are consistent with free TBAF and HF_2^- (the latter assignment consistent with values provided in reference 13). The integration of the B-F -ate complex is 0.51 (relative to 3.00 for benzotrifluoride), suggesting reversible -ate complex formation.

5.3.4 Fluoride Addition to DMF Solvent

A 2-dram vial was charged with DMF-d_7 (0.5 mL) and TBAF$\cdot$3H_2O (14 mg, 44 μmol). Analysis by ^{19}F NMR spectroscopy revealed two resonances at -110.88 and -147.69 ppm (Figure S42). The former resonance is consistent with TBAF, while the latter resonance arises from HF_2^- (the latter assignment consistent with values provided in reference 13).

6 NMR Data

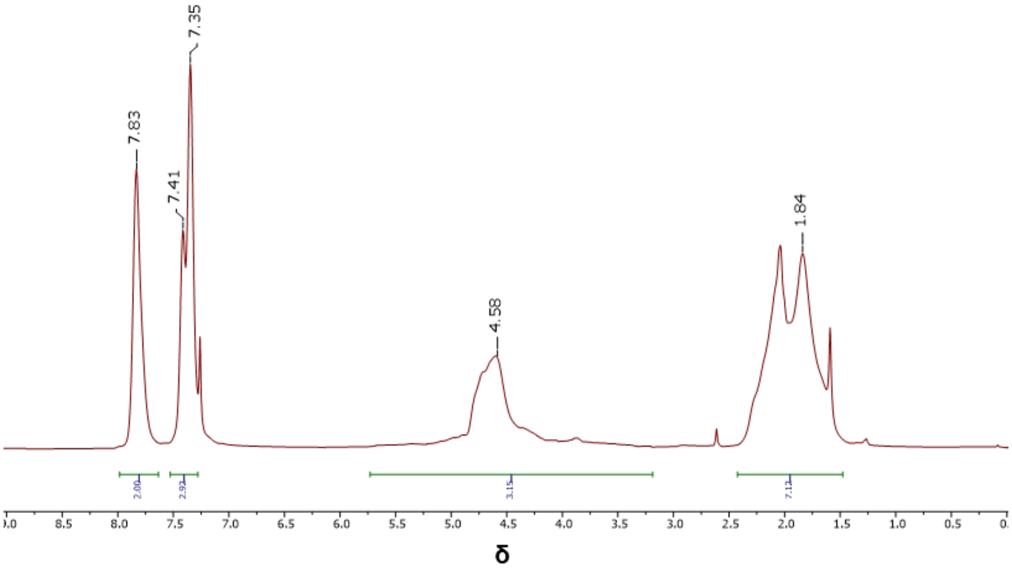

Figure S21: ^{1}H NMR Spectrum for Polymer **4_H** in $CDCl_3$

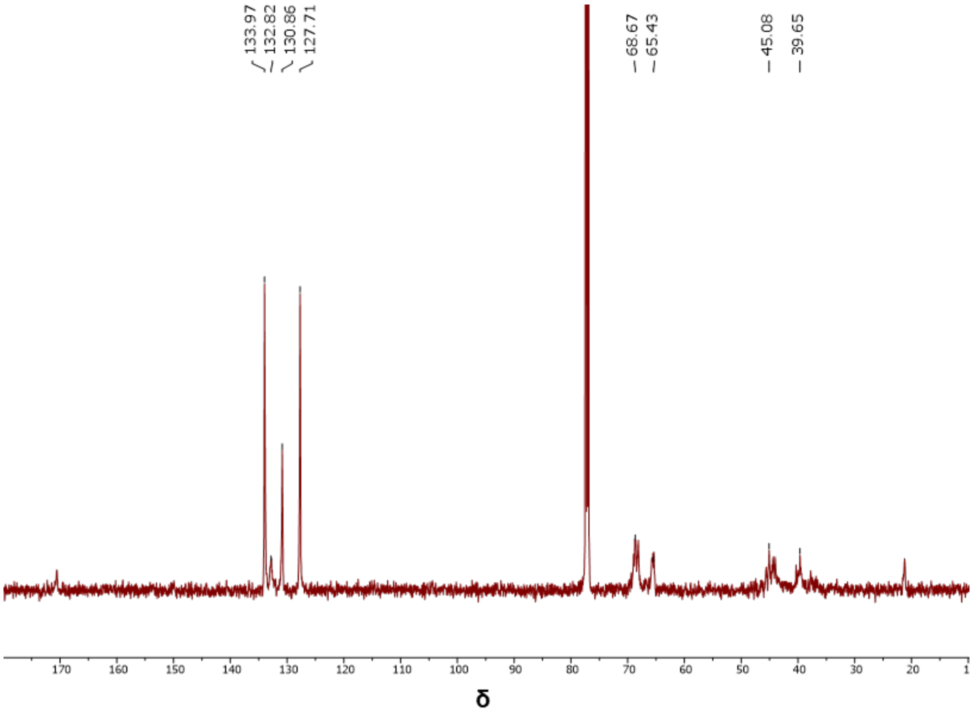

Figure S22: ^{13}C NMR Spectrum for Polymer **4_H** in CDCl3

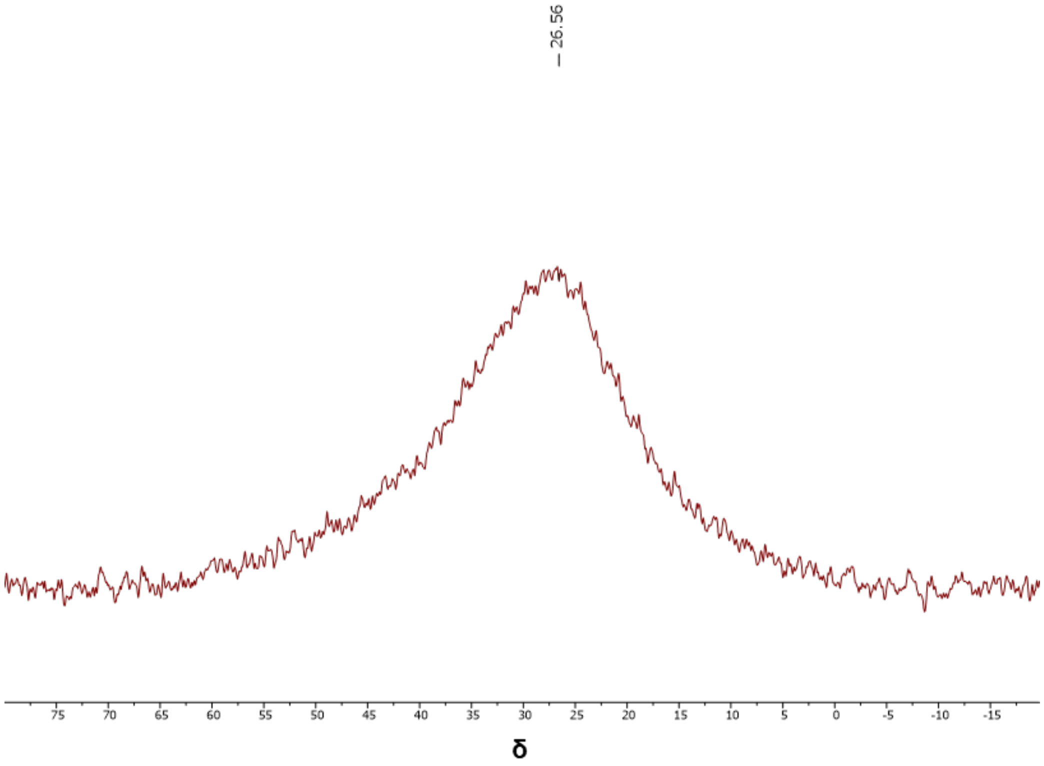

Figure S23: ^{11}B NMR Spectrum for Polymer **4$_H$** in CDCl3

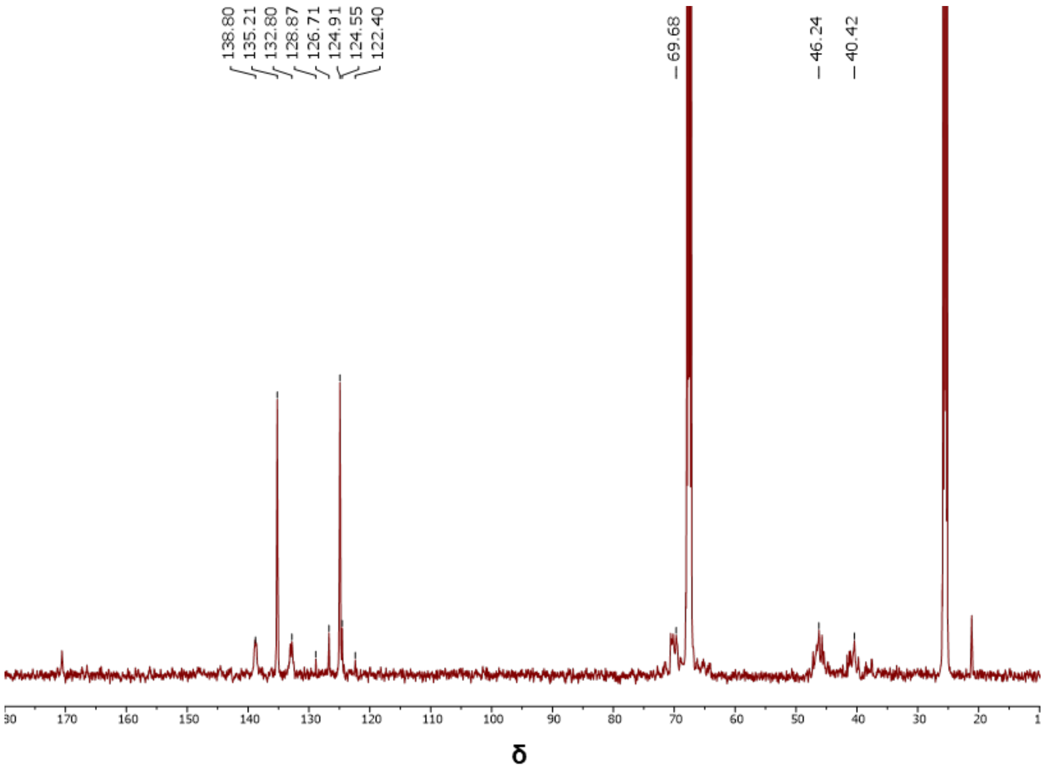

Figure S24: ^{13}C NMR Spectrum for Polymer **4$_{CF3}$** in D$_8$-THF

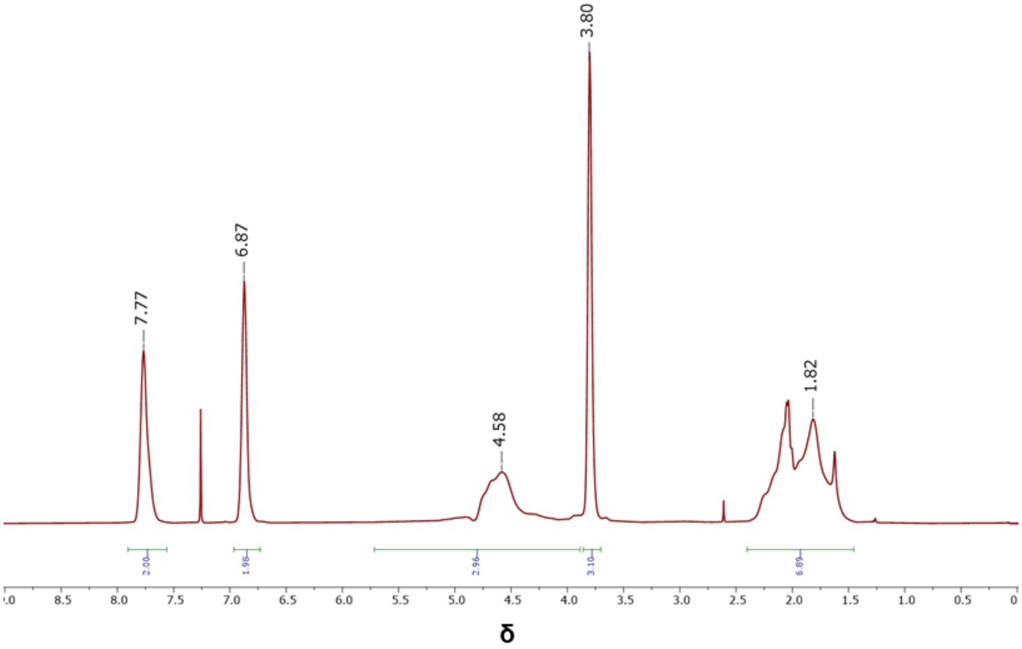

Figure S25: ^{1}H NMR Spectrum for Polymer **4$_{\mathbf{OMe}}$** in CDCl3

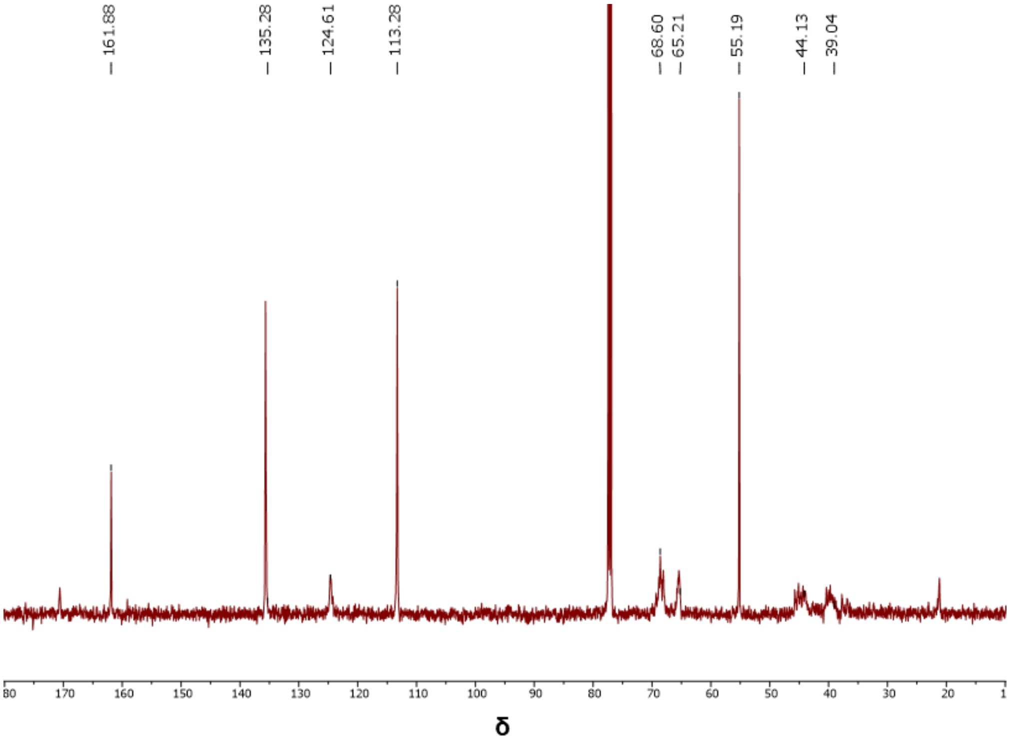

Figure S26: ^{13}C NMR Spectrum for Polymer **4$_{\mathbf{OMe}}$** in CDCl3

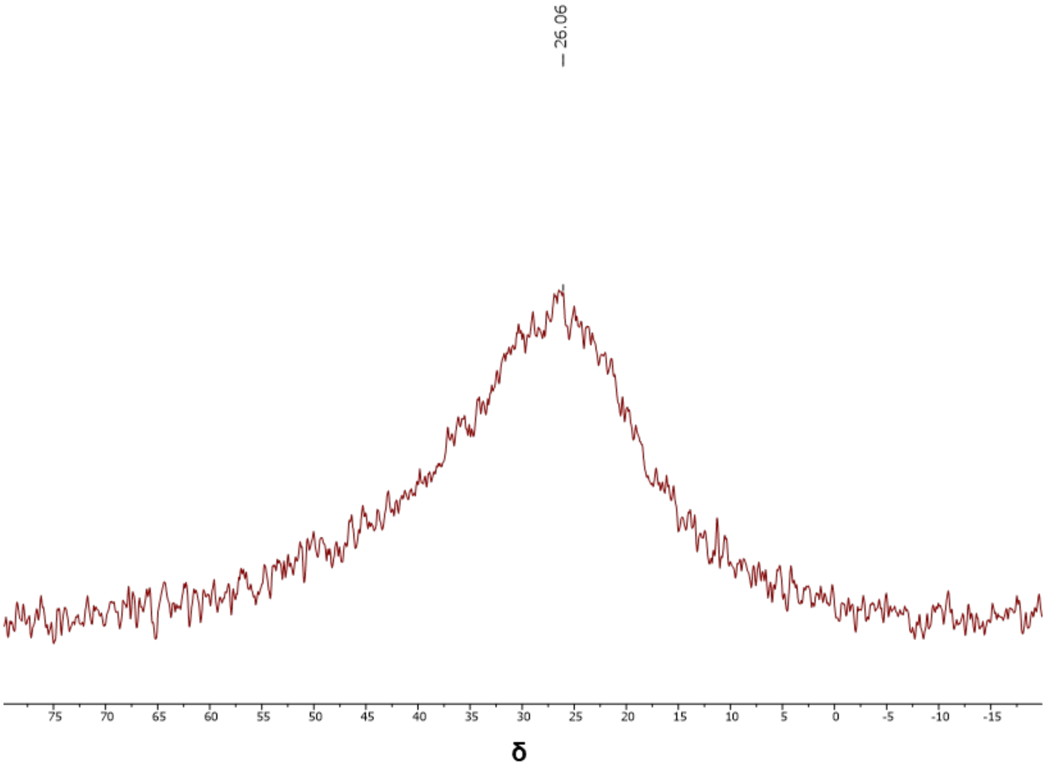

Figure S27: ^{11}B NMR Spectrum for Polymer $\mathbf{4_{OMe}}$ in CDCl3

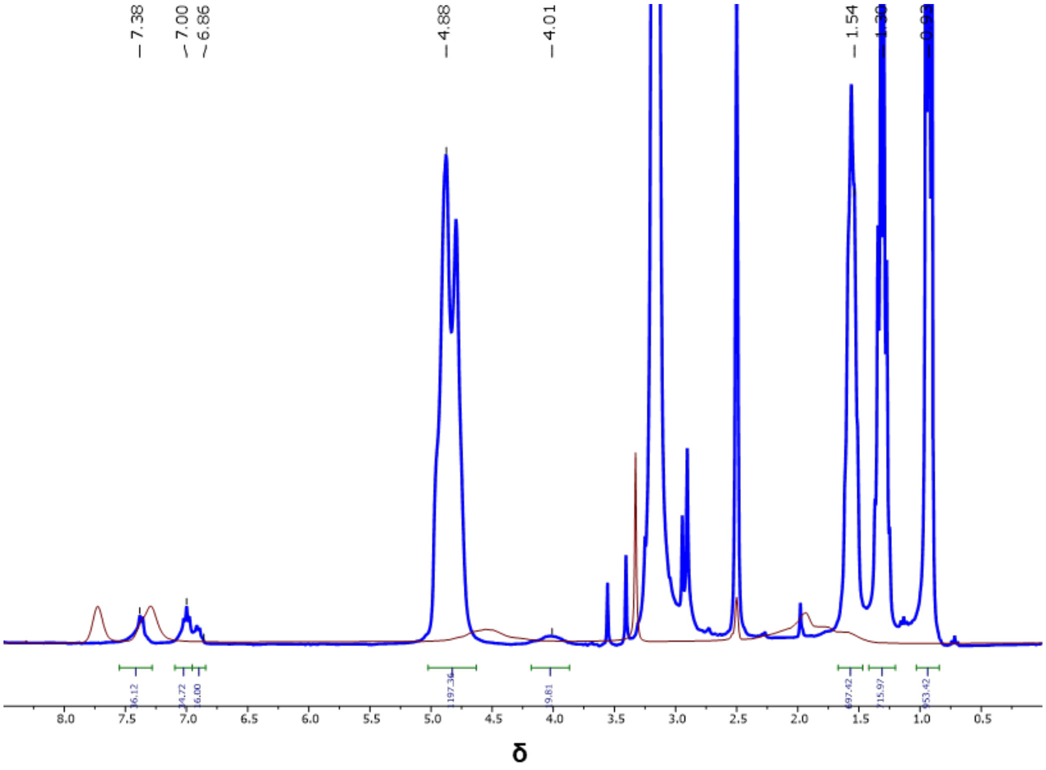

Figure S28: ^{1}H NMR Spectrum of Stoichiometric Hydroxide Addition to $\mathbf{4_H}$ in D_6-DMSO. Starting polymer solution (red) overlaid with polymer matrix and four equiv. TBAOH (blue)

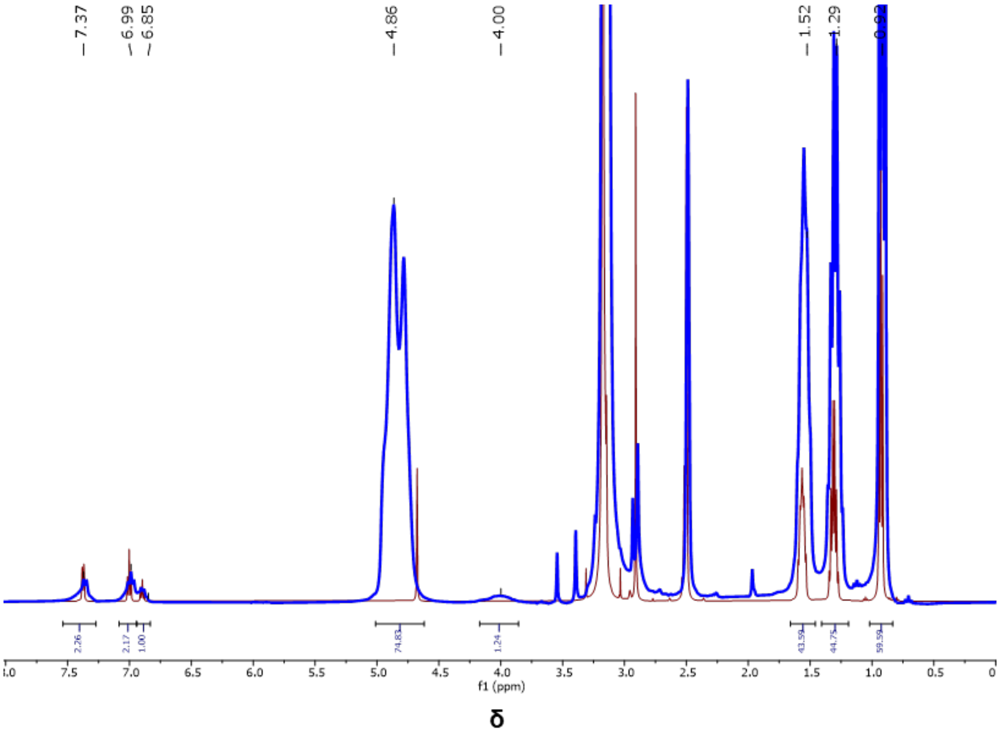

Figure S29: ^{1}H NMR Spectrum of Stoichiometric Hydroxide Addition (2 equiv.) to **PBA** in D_6-DMSO. Resultant boronate solution (red) overlaid with **4$_H$**/TBAOH mixture (blue) from Section 4.1.1.

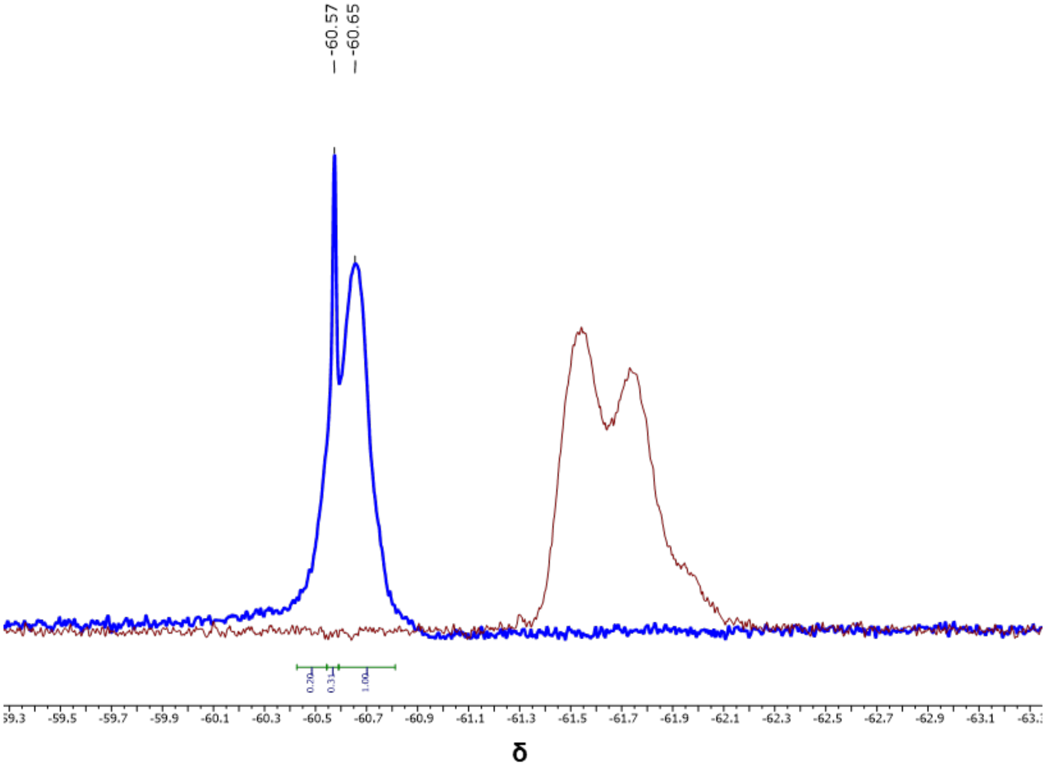

Figure S30: ^{19}F NMR Spectrum of Stoichiometric Hydroxide Addition to **4$_{CF3}$** in D_6-DMSO. Starting polymer solution (red) overlaid with polymer matrix and four eq TBAOH (blue)

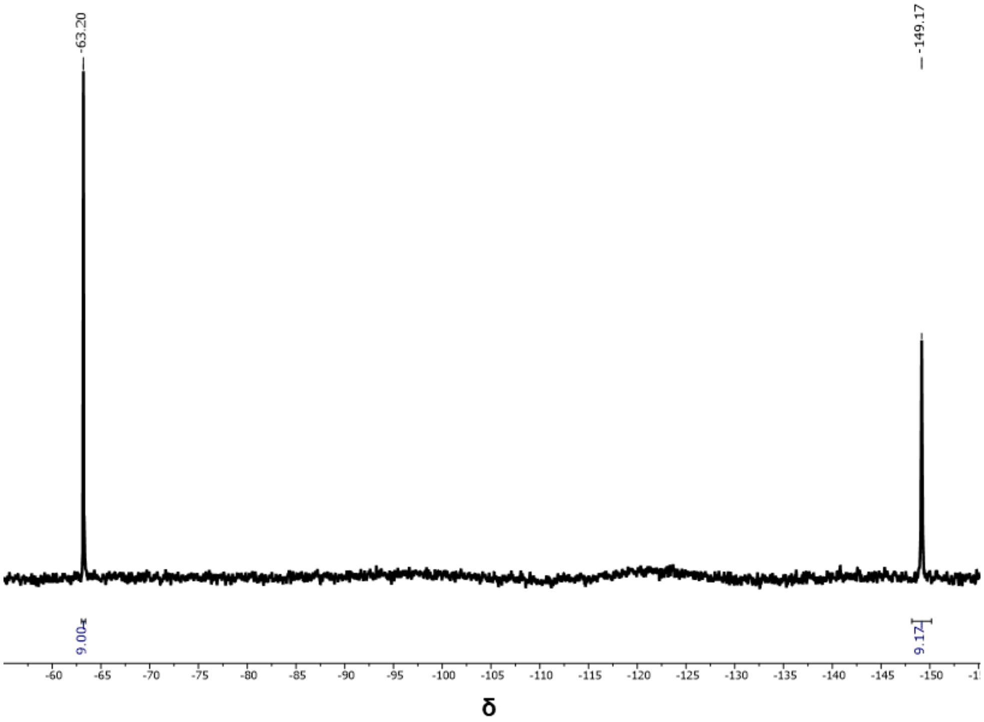

Figure S31: ^{19}F NMR Spectrum of Recycling Experiment with First Methanol Mixture (t_0)

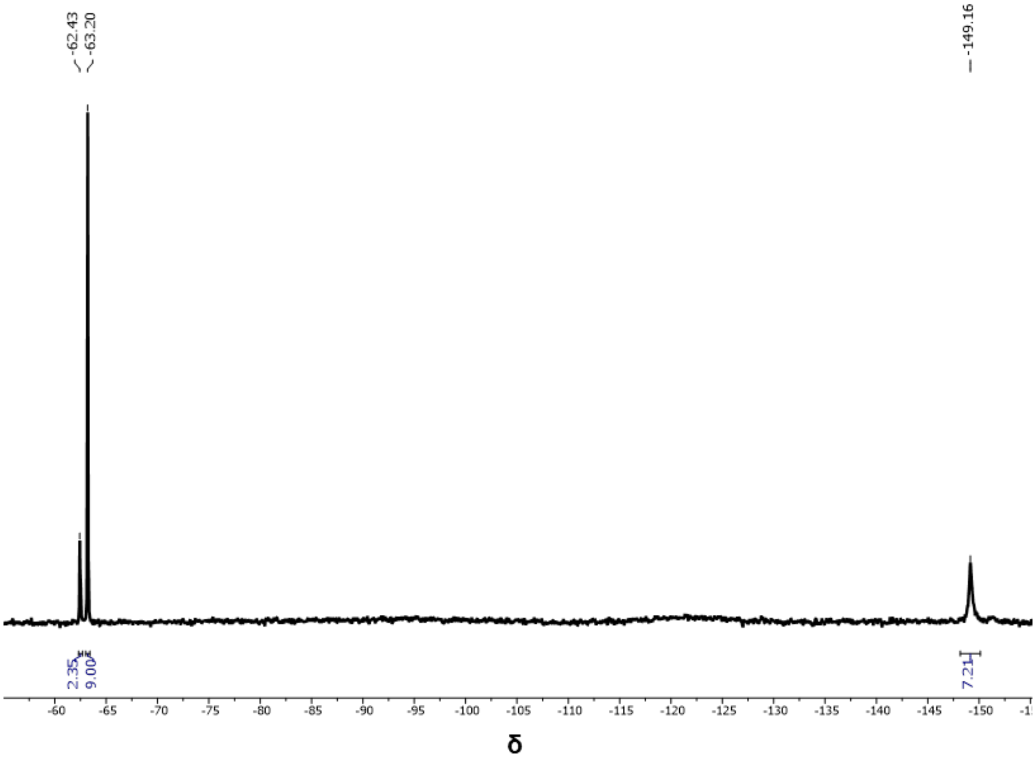

Figure S32: ^{19}F NMR Spectrum of Recycling Experiment with First Methanol Mixture (t_{24})

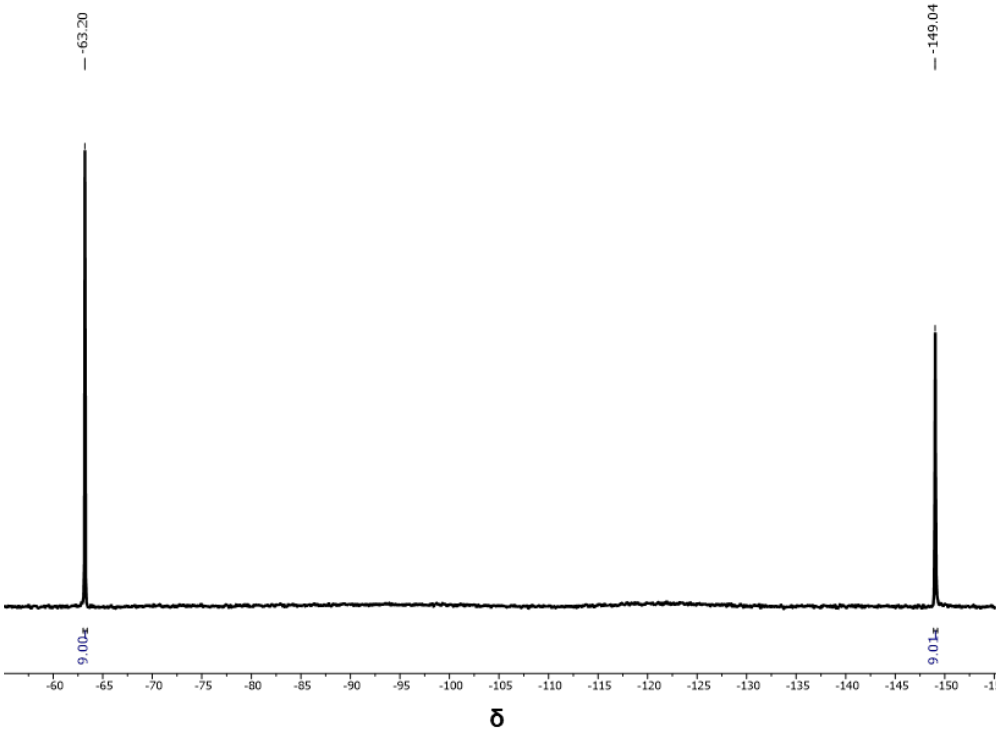

Figure S33: ^{19}F NMR Spectrum of Recycling Experiment with Second Methanol Mixture (t_0)

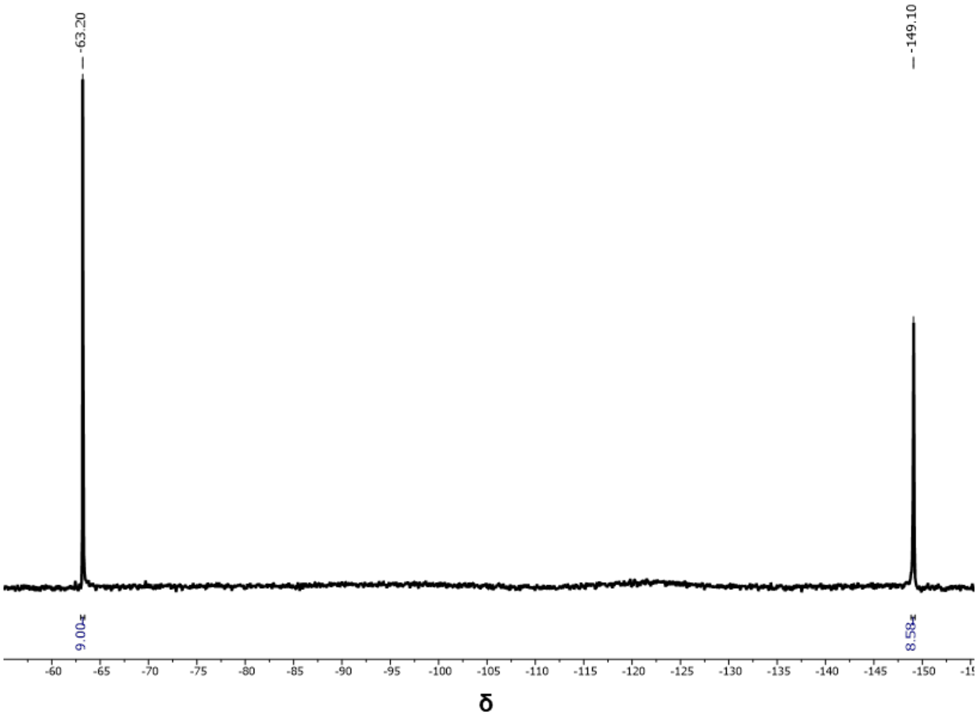

Figure S34: ^{19}F NMR Spectrum of Recycling Experiment with Second Methanol Mixture (t_{24})

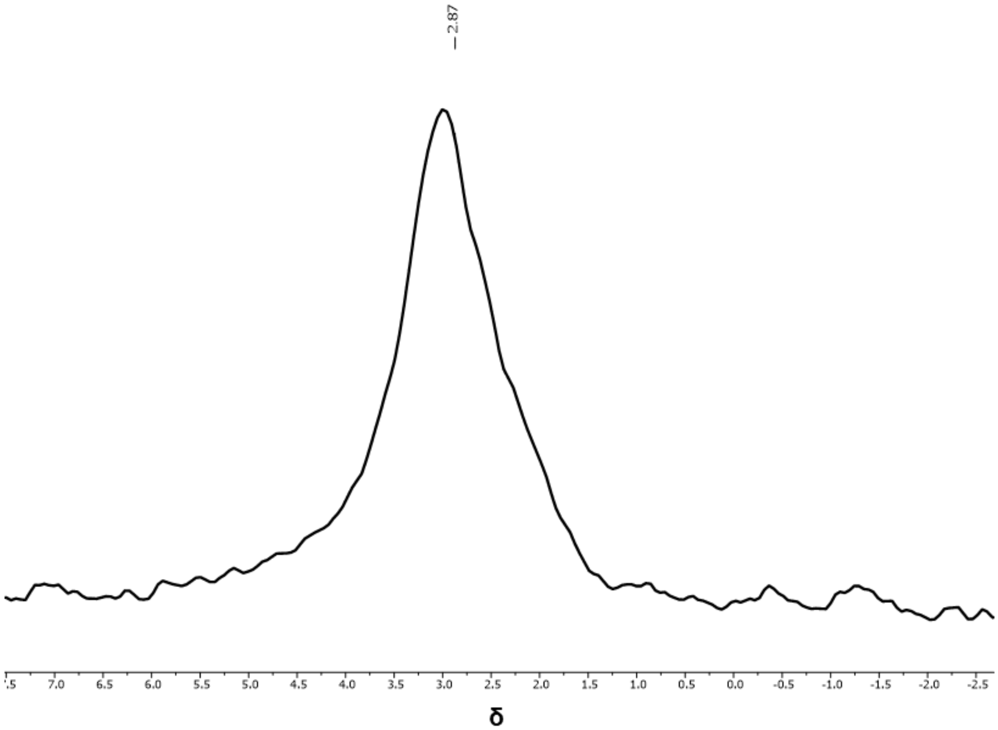

Figure S35: ^{11}B NMR Spectrum of Recycling Experiment with First Methanol Mixture (t_{24})

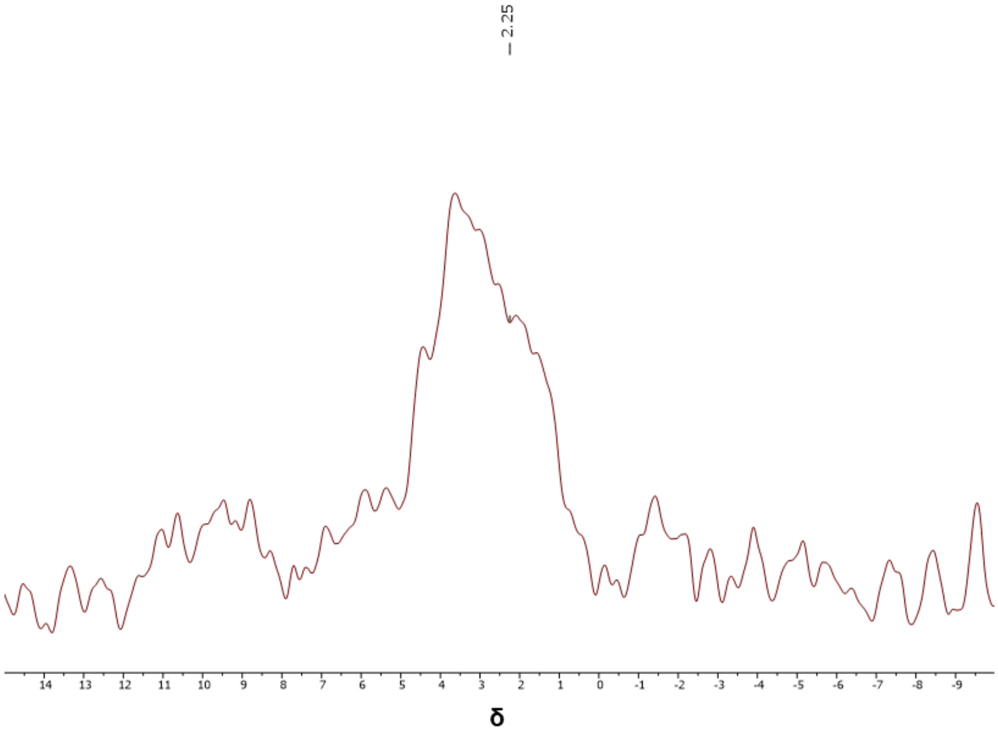

Figure S36: ^{11}B NMR Spectrum of Fluoride Addition to **4$_{CF3}$** in D$_6$-DMSO

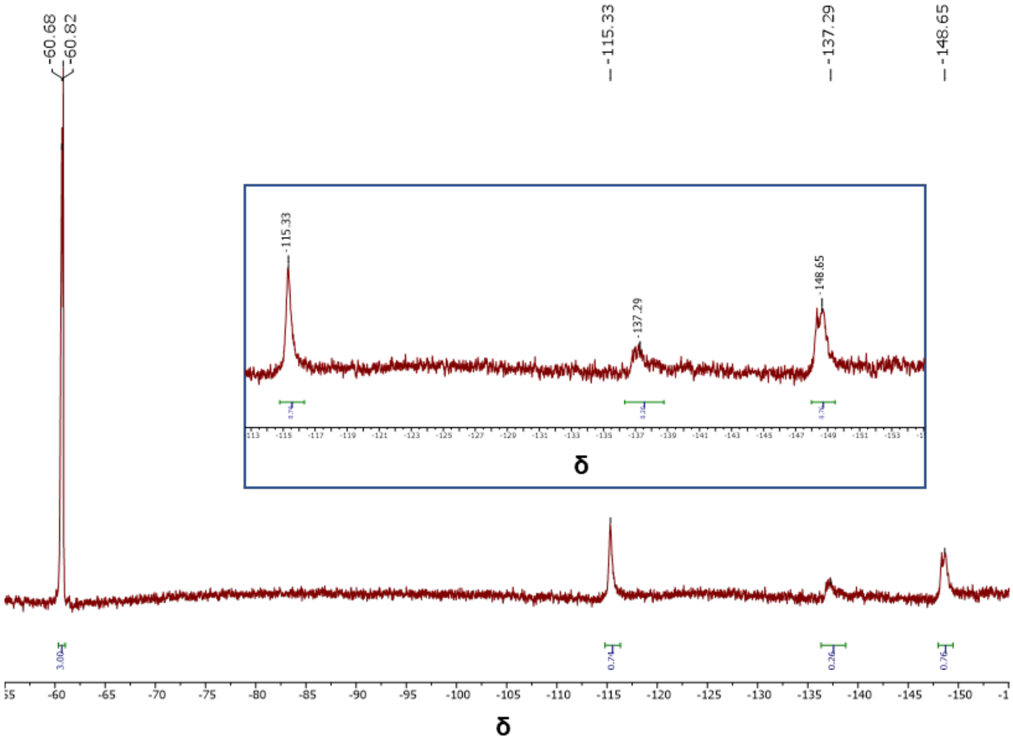

Figure S37: ^{19}F NMR Spectrum of Fluoride Addition to **4_{CF3}** in D_7-DMF. Upfield resonances provided in inset

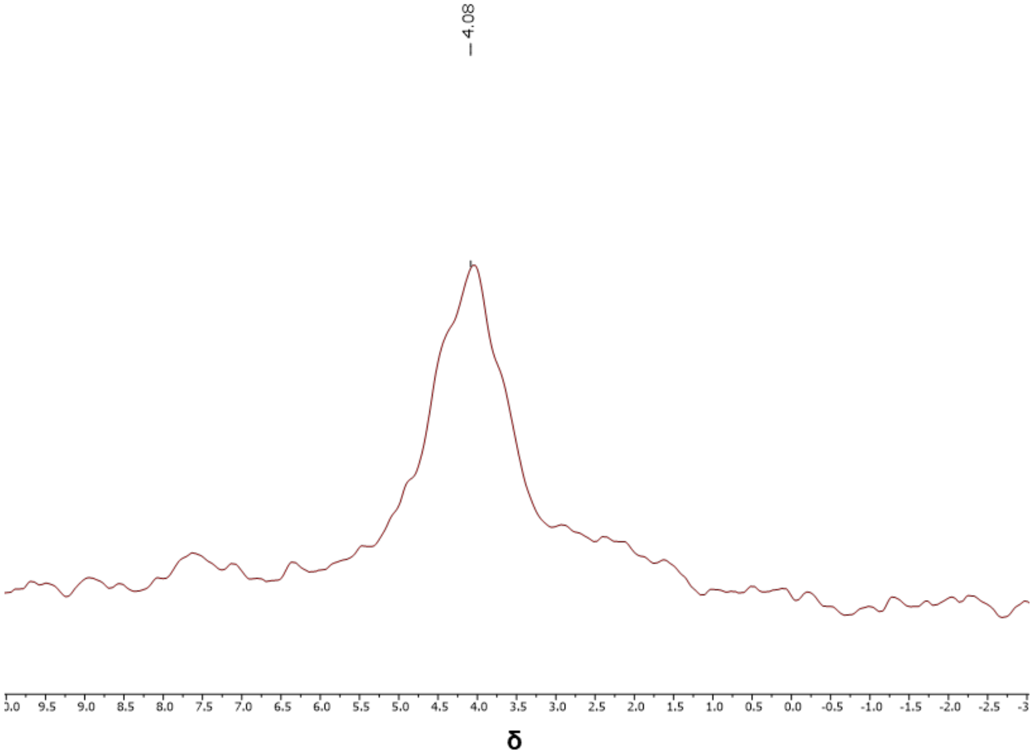

Figure S38: ^{11}B NMR Spectrum of Fluoride Addition to **4_H** in D_6-DMSO

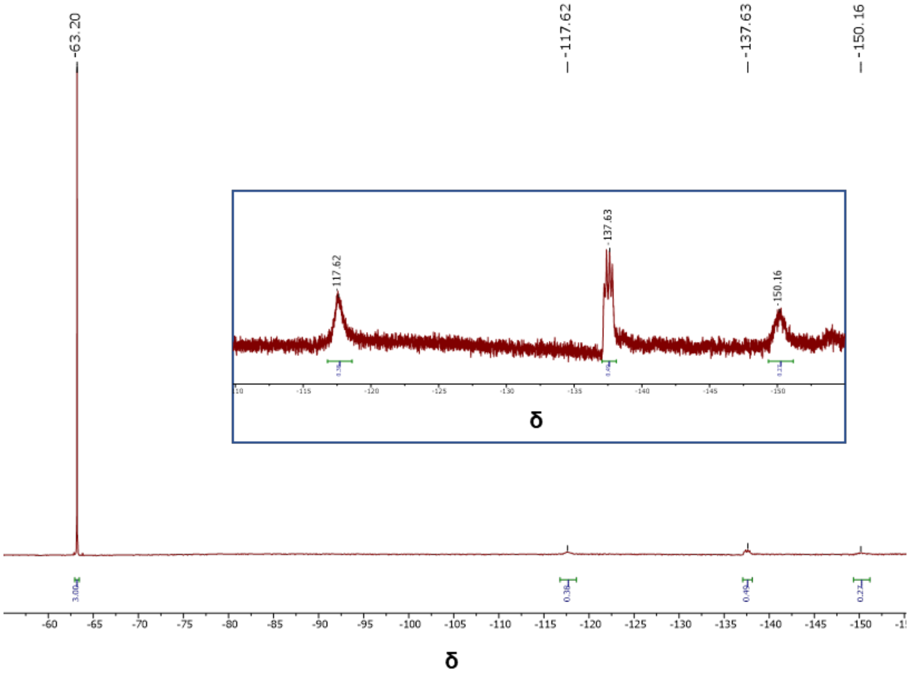

Figure S39: ^{19}F NMR Spectrum of Fluoride Addition to $\mathbf{4_H}$ in D_7-DMF. Upfield resonances provided in inset

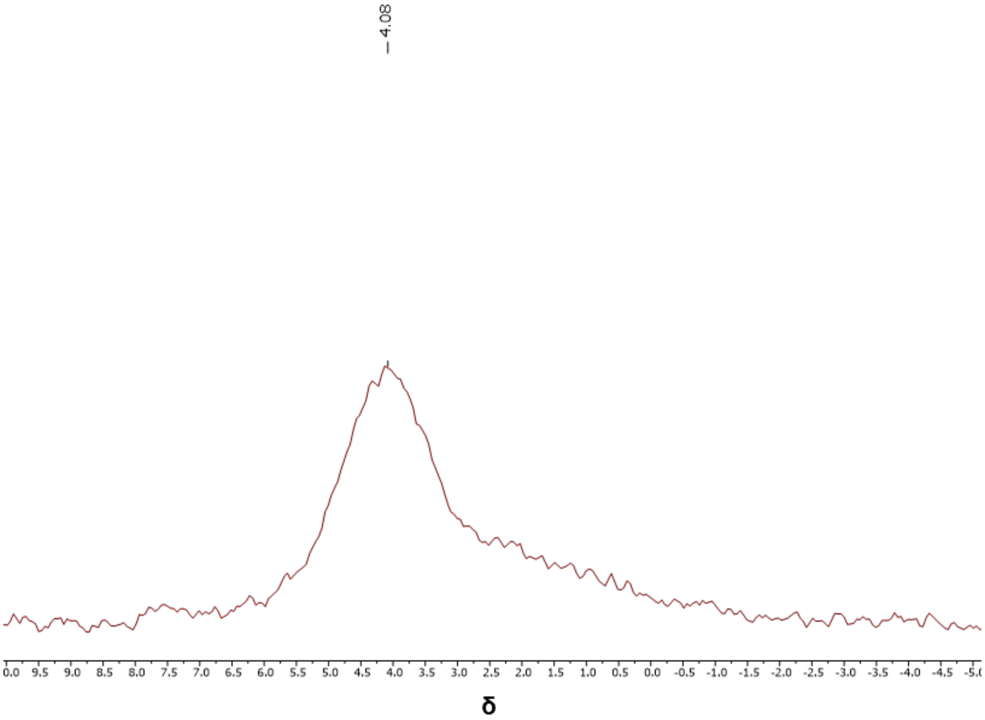

Figure S40: ^{11}B NMR Spectrum of Fluoride Addition to $\mathbf{4_{OMe}}$ in D_6-DMSO. Upfield resonances provided in inset

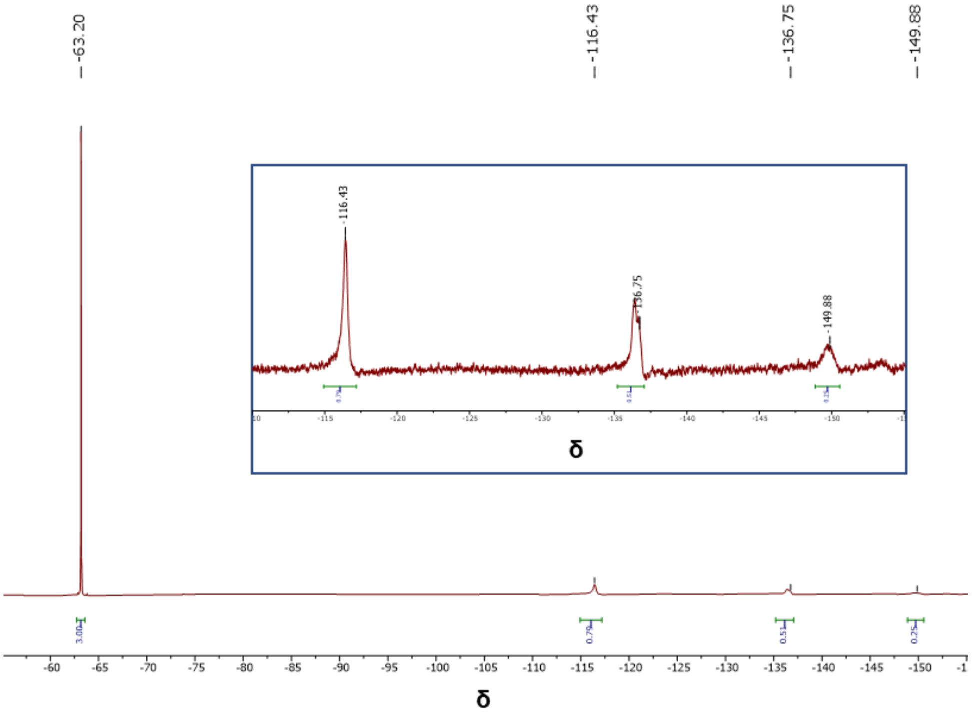

Figure S41: ^{19}F NMR Spectrum of Fluoride Addition to $\mathbf{4_{OMe}}$ in D_7-DMF. Upfield resonances provided in inset

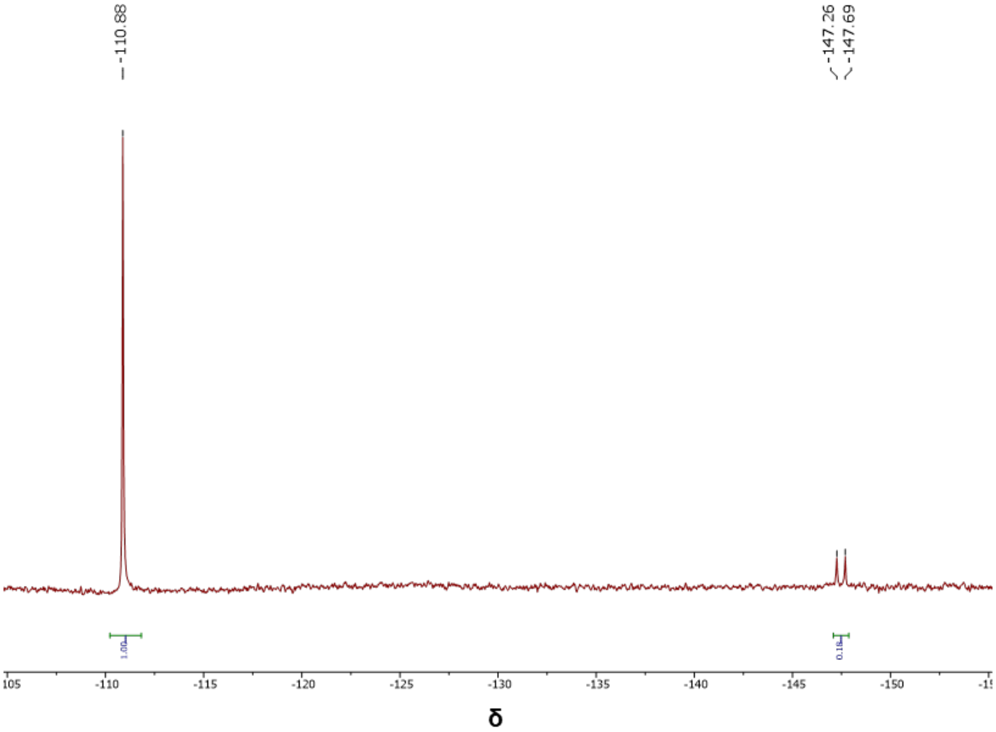

Figure S42: ^{19}F NMR Spectrum of Fluoride Addition to DMF Solvent

7 <u>Computational Methods</u>

7.1 Computational Details

Quantum chemical calculations were performed on saturated repeating units of $\mathbf{4}_{\mathbf{CF_3}}$ and fluorine to elucidate the atomistic effects of anion binding in **PVA**-aryl boronate polymers. All calculations were performed using the Orca 4.1 program package.[1] Density functional theory (DFT) geometry optimizations were performed at the B3LYP[2]/def2-SVP[3] level of theory with Grimme's "D3" dispersion correction[4] with the Becke-Johnson damping function.[5] Single point calculations were performed with the def2-TZVPPD basis set in order to obtain higher accuracy.[3,6] An ultrafine grid was used for integral evaluation (Grid6 setting). The resolution of identity was used in the computation of two electron integrals,[7] and the "chain of spheres" approximation was applied for the exchange integrals.[8,9] Frequency calculations were performed to ensure the optimized structures were minima on the potential energy surface. For reducing the computational complexity, TBAF was modeled as tetramethylammonium fluoride (TMAF).

Time-dependent density functional theory (TD-DFT) calculations were performed on the optimized structures to improve the interpretation of the observed UV-vis spectra. TD-DFT calculations were performed with the range-separated exact exchange CAM-B3LYP[10] functional and def2-TZVPPD[3,6] basis set to generate UV-vis spectra with 150 optimized roots, which has shown to be an accurate method in the calculation of excitation energies.[11] The orca_mapspc program was used to generate UV-vis spectra with 2000 cm^{-1} of peak broadening.

7.2 Fluoride Binding

The interaction energy between the repeating unit, henceforth referred to as a monomer (*Mon*), and the first TMAF was computed by using the following expression:

$$\Delta\mathrm{E}_{\mathrm{Mon-Pair}} = \mathrm{E}_{\mathrm{Mon-TMAF}} - \mathrm{E}_{\mathrm{Mon}} - \mathrm{E}_{\mathrm{TMAF}}$$

Where $\mathrm{E}_{\mathrm{Mon-TMAF}}$ represents the energy of the interaction supersystem, and $\mathrm{E}_{\mathrm{Mon}}$ and $\mathrm{E}_{\mathrm{TMAF}}$ correspond to the energies of the isolated systems. Therefore, $\Delta\mathrm{E}_{\mathrm{Mon-Pair}}$ describes the additional interaction energy over the cation-anion pair and the repeating unit of the polymeric material. The isolated monomer is planar with an intramolecular hydrogen bond as shown in Figure S43. Upon introducing the cation-anion pair TMAF, the fluorine binds to the boron, which yields a tetrahedral boron. The cation is found to interact favorably with the ether oxygen atoms, as it is shown in Figure S44. The interaction energy, $\Delta\mathrm{E}_{\mathrm{Mon-TMAF}}$, is considerable at -33.4 kcal mol^{-1}.

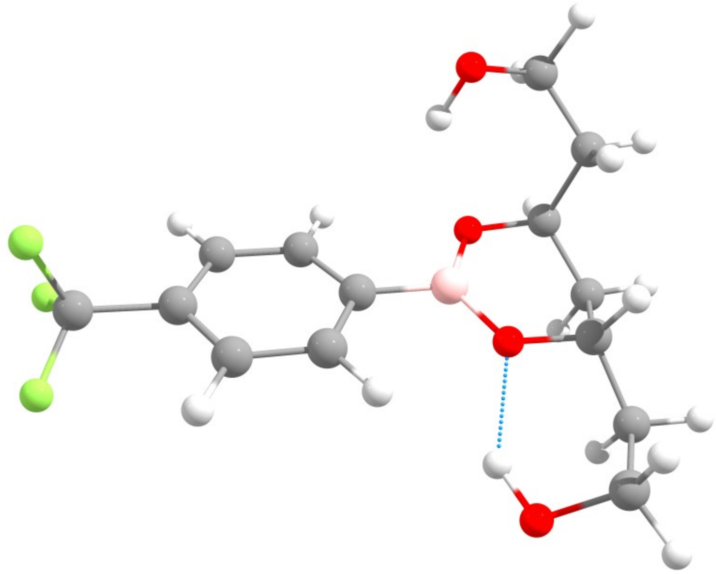

Figure S43: Optimized repeating unit. Color code: B (pink), O (red), C (grey), F (green), H (white)

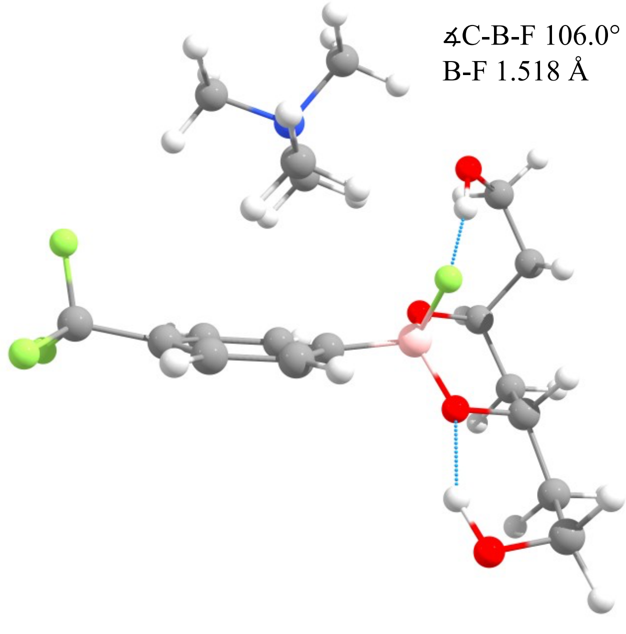

Figure S44: Optimized repeating unit + TMAF. The B-F bond length is 1.518 Å and is further stabilized by intramolecular hydrogen bonding from the neighboring hydroxy unit. Color code: B (pink), O (red), C (grey), F (green), H (white)

Upon addition of a second cation-anion pair (TMAF), the fluorine hydrogen bonds with the hydroxyl group of the monomer, granting an additional -23.7 kcal mol^{-1} over the $\Delta E_{\mathrm{Mon-TMAF}}$, calculated as:

$$\Delta E_{\text{Mon-2TMAF}} = E_{\text{Mon-2TMAF}} - E_{\text{Mon-TMAF}} - E_{\text{TMAF}}$$

The third equivalent of TMAF results in an additional -16.5 kcal mol^{-1}. This value was calculated by subtracting the energy of the monomeric unit that has two bound TMAF molecules:

$$\Delta E_{\text{Mon-3TMAF}} = E_{\text{Mon-3TMAF}} - E_{\text{Mon-2TMAF}} - E_{\text{TMAF}}$$

The binding of the second and third fluorine equivalent occurs is of similar nature, i.e. at hydroxo sites of the polymeric material. For that reason, we have also considered an average interaction between the Mon-TMAF supersystem (first fluorine equivalent bound on boron) and two cation-anion pairs as:

$$\Delta E'_{\text{Mon-3TMAF}} = E_{\text{Mon-3TMAF}} - E_{\text{Mon-TMAF}} - 2E_{\text{TMAF}}$$

The $\Delta E'_{\text{Mon-3TMAF}}$ is -40.2 kcal mol^{-1}, with an average of -20.1 kcal mol^{-1} per TMAF, which is in agreement with the average of $\Delta E_{\text{Mon-2TMAF}}$ and $\Delta E_{\text{Mon-3TMAF}}$ when binding of the second and third TMAF is separately considered, respectively:

$$((-23.7 \text{ kcal mol}^{-1}) + (-16.5 \text{ kcal mol}^{-1}))/2 = -20.1 \text{ kcal mol}^{-1}$$

No additional binding sites were for fluorine were located, and therefore we conclude that the monomer can effectively capture multiple fluoride units at the boron sites and hydroxy units, which is consistent with experimental observations.

7.3 Calculated UV-vis Absorbance Spectra

TD-DFT calculations were performed on a repeating unit of $\mathbf{4_{CF_3}}$. The scope of these calculations is not to reproduce the experimental spectra, since they have been performed on a gas-phase, isolated molecular model and they do not capture the properties of the bulk, amorphous material. For example, effects from π-π stacking between two repeating units are neglected. Such effects are expected to red-shift the TD-DFT transitions with respect to the experimental results.[12] However, these calculations offer a description on the electronic structure of the ground and the first, low-lying states, which can explain qualitatively the changes of the experimental UV-Vis spectra.

The calculated UV-vis spectra for the monomer and transition electron density differences are shown in Figure S45. Table S2 shows the molecular orbital contribution to the first two excitations. Overall, the leading excitations for both peaks correspond to excitations from the conjugated π ring to the electron deficient atomic p orbital of boron, which is part of the conjugated π system of the molecular unit. Herein, the focus is on the peak labeled **1**, because the peak in this region experimentally exhibits increased ratiometric absorbance upon addition of tetrabutylammonium fluoride, and is the targeted excitation for the observation of fluorescence.

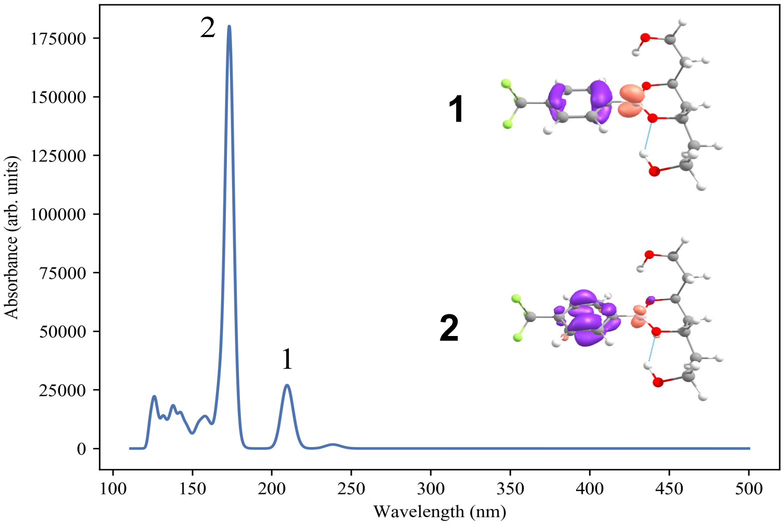

Figure S45: Calculated UV-vis spectra for repeating unit at the CAM-B3LYP/def2-TZVPPD level of theory. Inset: Electron density differences of the electronic transition between the ground state and the two excited states. Purple isosurface corresponds to electron deficiency of the molecule related to the ground state, pink isosurface to electron excess. Both 1 and 2 correspond to excitations from the aromatic π orbitals to the empty 2p orbital of boron. Color code: B (pink), O (red), C (grey), F (green), H (white)

Table S2: Transition energies (in eV) and the corresponding molecular orbital contribution to the first and second peaks in Figure S38

State	Energy	Transition		Weight
1	5.92	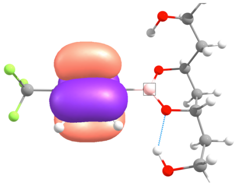 HOMO	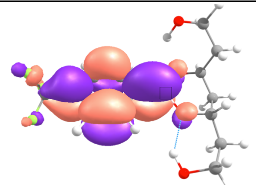 LUMO	65%
		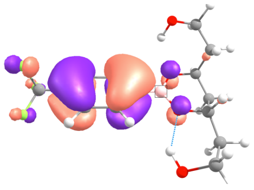 HOMO-1	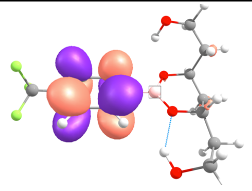 LUMO-1	22%

2	6.86	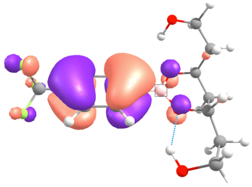 HOMO-1	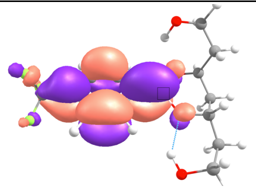 LUMO	76%
		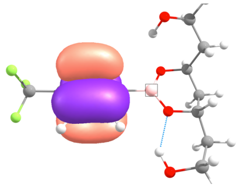 HOMO	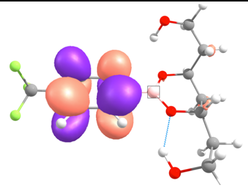 LUMO-1	14%

The spectra of the monomeric unit were calculated with the presence of one and two TMAF units and are shown in Figure S46. Both spectra contain a strong peak characteristically equivalent to the unsaturated monomer (Figure S45) at approximately 6.9 eV. Although the excitations seem equivalent to those found for the unsaturated monomer, the nature of the excitations are not synonymous. For 1-TMAF and 2-TMAF, the π-π* excitation is mainly localized to the phenyl group (see Table S3).

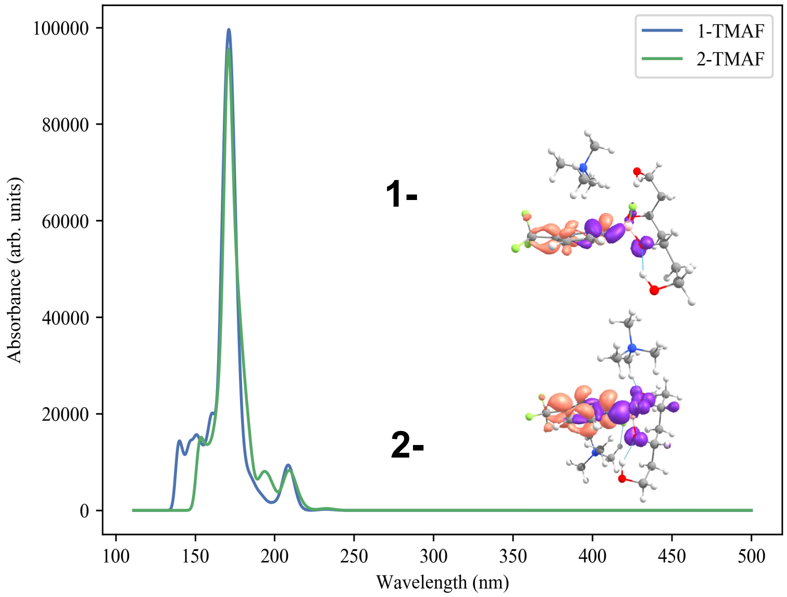

Figure S46: Calculated UV-vis absorbance spectra with one (blue) and two (green) TMAFs added to the repeating unit at the CAM-B3LYP/def2-TZVPPD level of theory. Both spectra show a characteristic peak at approximately 215 nm.

Table S3: Transition energies (in eV) and the corresponding molecular orbital contribution to the first peaks shown in Figure S39

Molecular System	Energy	Transition		Weight
1-TMAF	5.95	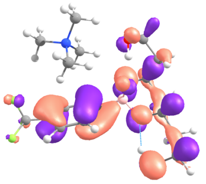 HOMO	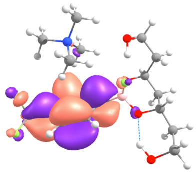 LUMO	48%
		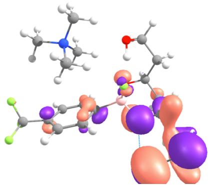 HOMO-1	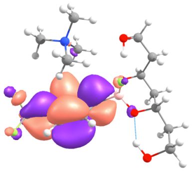 LUMO	14%
2-TMAF	5.96	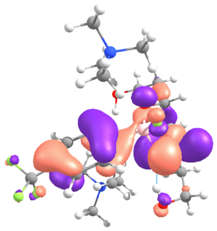 HOMO-1	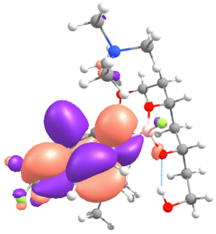 LUMO	33%
		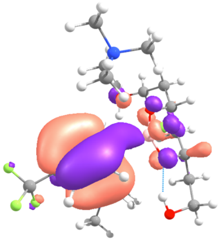 HOMO	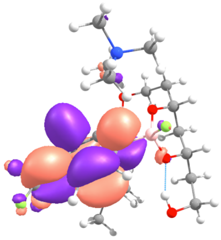 LUMO	14%

When comparing the calculated to the experimental spectra in Figure 3 (main text), the bare polymer does not show a strong characteristic peak corresponding to Peak 1 in Figure S45. Additionally, the presence of solvent and other polymeric units may donate electron density to the boron atom, reducing the prevalence of this peak. However, the presence of peaks after the addition of the fluorine correspond to polymer backbone to π* excitations in the material. Increasing the equivalents of fluorine did not increase the intensity of these peaks, suggesting that the ratiometric increase in absorbance is due to increased fluorine occupancy of the boron sites, since there are many competitive binding sites with strong interactions (cations and hydroxyl units).

7.4 Cartesian Coordinates

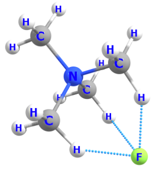

Coordinates from ORCA-job orca

C	3.63104706564139	-0.35020676490833	-2.07597982766934
N	3.84598417615583	1.07757073165269	-1.65374830625025
C	2.62485830737094	1.86879805329437	-2.04199500288607
C	3.97930468902465	1.11166084251119	-0.15340260252947
C	5.05988416254048	1.64037944044208	-2.29739144546790
H	5.18833044816284	2.66896570009133	-1.96970448467336
H	5.92507983521012	1.05065260505154	-2.00427116045640
H	4.94057388202886	1.60999605304449	-3.37769688829270
H	4.50318540544967	-0.92893460765770	-1.77951636098083
H	2.72017315951827	-0.67049338520890	-1.55230311895409
H	3.51918215511649	-0.37216785938199	-3.15798093514989
H	2.77363819322494	2.89841837120942	-1.72438642919853
H	2.52124667715406	1.82130894880032	-3.12405446015588
H	1.79201262200216	1.38212548438241	-1.50927681663306
H	4.11925238310810	2.14686910019447	0.14973025723279
H	3.03231968903903	0.68557324771606	0.22169758296418

H	4.84913768727527	0.51885140445739	0.12145001561208
F	1.45764346197688	0.04338873430915	-0.31579101651129

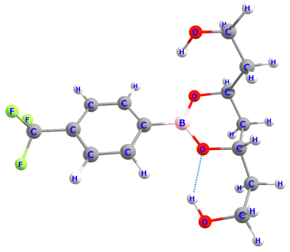

Coordinates from ORCA-job orca

C	-0.11706071838961	0.65306083573625	1.88030196534745
C	0.84065926858911	1.45055791622409	2.53355752202082
C	1.72859360339476	2.24701733411203	1.81162079754091
C	1.67002581396979	2.25757548974245	0.41335918991722
C	0.72491616658342	1.47323310003165	-0.25808163022510
C	-0.15520102202328	0.67772667793963	0.47436590378683
C	2.65884594384115	3.07897962654276	-0.37439239493504
F	3.76887919463227	2.37097220374322	-0.66163873655760
B	-1.10945930501984	-0.23858827161442	2.69419308589226
O	-1.20213200566930	-0.05462042487332	4.04514842608967
C	-2.04951857036720	-0.87034230888449	4.87502195485372
C	-2.48896347622741	-0.05017195805300	6.08364337282340
C	-1.33147321665313	0.66283585999737	6.79113843874234
O	-0.86463774430853	1.78400366779460	6.08065129401550
F	2.14555187704492	3.49311664272807	-1.54660846889623
F	3.05315903310760	4.17142749763371	0.30298323416551

O	-1.85511485268675	-1.17761089144064	2.03771393119044
C	-2.71599642976282	-2.08066740535274	2.75720958111630
C	-3.20732951827802	-1.41443896245067	4.04413454774730
H	0.89306763167695	1.44589160729933	3.62536926676592
H	2.46352612855644	2.86602330603097	2.32923894258567
H	0.67775825899955	1.49503271111896	-1.34835650651251
H	-0.89595721240790	0.06958147535857	-0.05097571767572
H	-3.57687414477375	-2.25546569977701	2.09048199920296
H	-1.42215448965939	-1.70623282665723	5.23346660806883
H	-3.88155421912315	-0.58039063778079	3.78554019648401
H	-3.79030980628064	-2.13366020624125	4.64046615627769
H	-2.99663338716195	-0.73239984664721	6.78719677866203
H	-3.22715823130143	0.70908757070269	5.77181014704613
H	-1.67393213348657	1.02442452655097	7.77466457989339
H	-0.51999114327834	-0.07146324672014	6.99043789182393
H	-0.75609486678188	1.49468864430481	5.16247053489035
C	-2.00162137707754	-3.41559371302931	2.97309600468751
H	-1.17225058426739	-3.29432074570478	3.69093590848378
H	-2.72641693288730	-4.11501789883986	3.42558841810965
C	-1.43871783098599	-4.03102870580045	1.68837014025342
H	-1.11156923169648	-5.06231444632114	1.89830252533803
H	-2.25301243600770	-4.10540958202676	0.93482072982724
O	-0.31790809448375	-3.34608421234117	1.18477055445355

H	-0.59292976534894	-2.43007752903577	1.03518110569844

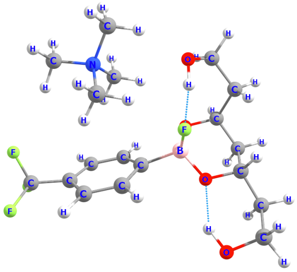

Coordinates from ORCA-job orca

C	-0.36979896686364	0.70048098384803	1.46784820745654
C	0.99739616792648	1.02374666370649	1.53393871726637
C	1.58397725508100	1.91658952923315	0.63432751334664
C	0.79481739121794	2.52236742068615	-0.35360577458985
C	-0.58801009372323	2.29532428899060	-0.37492247265447
C	-1.15281460946773	1.39926894627143	0.53495841656172
C	1.42881424893737	3.30183850842252	-1.46460266058730
F	1.63777882609506	2.49927165740265	-2.55533786284834
B	-0.99176752271486	-0.51049646087431	2.34400889297852
O	-0.98338783573112	-0.18695084877563	3.74591975952770
C	-1.75345175291592	-0.99350933030599	4.62106198348895
C	-1.72157415008124	-0.36616459649657	6.01374585905222
C	-0.29895768477141	-0.11511282769591	6.52330373370884
O	0.36316362405566	0.90108727831947	5.81427000483432
F	0.66014261126515	4.31437323202812	-1.89804249304836
F	2.62744263927675	3.80594623231286	-1.13720615335645

F	-0.06989817618976	-1.69781520826304	2.13200891250983
O	-2.28296941749536	-0.90288461581054	1.81280257991403
C	-3.15725755958142	-1.66592285669080	2.61692454487574
C	-3.17032479603166	-1.14209940875434	4.06116464529205
C	0.39645250345542	-0.98602033083156	-3.26689554217019
N	-0.00996833092994	-1.63870357845909	-1.98459539890804
C	0.97752619488201	-1.25961693271847	-0.91549558860535
C	-0.03669859777156	-3.13109548940944	-2.13684444184196
C	-1.38058591313945	-1.16294539708599	-1.58480563413600
H	0.46562556007062	0.09798696490281	-3.10799642337255
H	-0.39992082314823	-3.55773566459268	-1.18918062321172
H	-2.09398881429493	-1.48798730393393	-2.35283741441571
H	1.95744089351546	-1.67060506576909	-1.18998172485142
H	1.62512284449295	0.52690905901290	2.27904904979708
H	2.65516254653583	2.12565188986019	0.67417205872999
H	-1.20843585673434	2.80673657580413	-1.11553744559921
H	-2.22494425837190	1.18891129004148	0.50305620816932
H	-4.16904460755844	-1.52752974572308	2.18907646340242
H	-1.28238334798477	-1.99681412554008	4.69297396009985
H	-3.64862483071779	-0.14848892041885	4.07495748330574
H	-3.76879713454494	-1.81018633038005	4.70330522122558
H	-2.25858520041683	-1.03039418295765	6.71397724888991
H	-2.26093793971459	0.59735428368833	5.98885602751293

H	-0.33614538956642	0.18789152092262	7.58503412894553
H	0.26323399672011	-1.07705582497047	6.49312024179352
H	0.14385417385045	0.73786089807401	4.87754737207013
H	0.97720956459114	-3.47832980914177	-2.37364783410115
H	-0.72077849358256	-3.38505945129288	-2.95711076579721
H	1.02868211083777	-0.16772465822859	-0.86326135679286
H	0.64464907469363	-1.65169443991156	0.05211400802343
H	-1.35360838810228	-0.07211638710798	-1.51033368208794
H	-1.62790938974367	-1.59938944286571	-0.60895870706597
H	1.37677595384351	-1.37590054245035	-3.56999766209417
H	-0.35003849207060	-1.21309459397920	-4.03858435334516
C	-2.86156736303787	-3.17809642704137	2.55196781695658
H	-1.98640380782048	-3.43579693960507	3.17269005750258
H	-3.72261839388194	-3.70853007581963	2.99470498730808
C	-2.62518847676070	-3.71835705392882	1.14255479299173
H	-2.79533970868547	-4.81048710298961	1.13291149339932
H	-3.37001586749778	-3.27268490055084	0.45079254663334
O	-1.31489689284002	-3.47639777957088	0.65586588908228
H	-0.85614990685945	-2.85890405058619	1.26946499882863

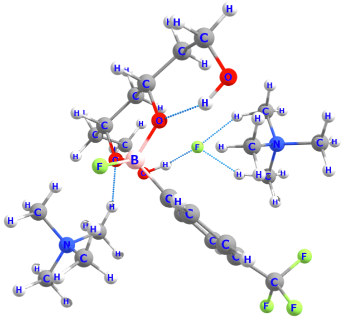

Coordinates from ORCA-job orca

C	0.73183586597296	-0.79799377797003	2.20005876029416
C	1.83544162716484	-0.10986514031109	2.73488435209051
C	2.28349830755277	1.09847696661578	2.19485370966249
C	1.64693995821106	1.62714032769189	1.06453853042628
C	0.58543665492404	0.92608102683234	0.47335324776912
C	0.13046286300397	-0.26004874981506	1.04821681008979
C	1.98654100771469	2.99755121040917	0.56913881287853
F	1.96785602839108	3.08852746728282	-0.77355583413312
B	0.09902214587832	-2.07559304092059	2.99529069066638
O	-0.56470164891316	-1.52221534293082	4.17695670713396
C	-1.69276004675750	-2.16824344308871	4.74122568627349
C	-2.35389679551744	-1.21762098805461	5.74361719538375
C	-1.37486659565798	-0.60073654974245	6.74375534790901
O	-0.44842684576793	0.27081169099670	6.12952139919966
F	1.07464031115887	3.91924672420568	1.01409861859313
F	3.18578921740237	3.43205727478995	0.98791480581789

F	1.17807177214412	-2.96270505210497	3.39476920241681
O	-0.78881941491672	-2.83870738908565	2.12093532269869
C	-1.91836089596849	-3.50719841012122	2.64669475427566
C	-2.64846973816357	-2.59835009859265	3.63167632856595
C	0.01120696857888	-3.16390866369534	-0.74065871269486
N	1.21633007860675	-3.99089019475673	-0.35792271589165
C	2.22354151052590	-3.14328786896454	0.37120014232150
C	1.83752896278284	-4.56075266640596	-1.58674859442293
C	0.77715729653621	-5.08956648114403	0.56604132539742
H	-0.47823591396680	-2.80252899069298	0.17401450042953
H	2.68836487898437	-5.19475614766156	-1.30515682324550
H	0.05203578252326	-5.72307854694619	0.04003926815202
H	2.37095253008548	-2.20870939914209	-0.18209032376996
H	2.33424752129462	-0.51548808797588	3.61996319790809
H	3.11327755710423	1.64123483115637	2.65278077569709
H	0.08740043786857	1.33747856692601	-0.40844151717212
H	-0.76459098674888	-0.74087896830410	0.65548100079768
H	-1.57377840250370	-4.40605729207986	3.20903953754853
H	-1.35140822511352	-3.06998406905578	5.29742545124448
H	-2.98657594688283	-1.69778739089628	3.09248101857287
H	-3.52003095605010	-3.12242282568914	4.06105514772684
H	-3.13748982243742	-1.77228093667101	6.28937069225392
H	-2.86100184065182	-0.40919712871388	5.18880428451914

H	-1.92778108280993	-0.01759021023774	7.50162519106149
H	-0.85443728730365	-1.41611349113869	7.29174786999450
H	-0.13763275385683	-0.23246055097452	5.34517626048291
H	2.18093739395971	-3.73677475913252	-2.22536305256291
H	1.08884052272064	-5.15633019168573	-2.12415524937670
H	1.85403331573212	-2.93487597205571	1.38223162915005
H	3.16365487596997	-3.70718957907788	0.43224813661961
H	0.31554267084581	-4.60762119207726	1.43868823407409
H	1.65787781536107	-5.67654409324510	0.85682357415903
H	0.34981418508734	-2.33058973427223	-1.36718515092461
H	-0.68129707580057	-3.80475108715935	-1.29859955139347
C	-2.80027166070308	-4.01730751401782	1.49958249135094
H	-3.53776505198821	-4.72246630145013	1.92636077391338
H	-2.16826944569371	-4.61721937322196	0.81988154230723
H	-4.16422336062339	-3.52631209174526	-0.07926708666422
C	-3.57410217179995	-2.97239961296916	0.68116968539224
H	-4.31299682175377	-2.48036458089440	1.34273629749350
O	-2.78303489612482	-2.01088447280375	0.04211161626730
H	-2.82414528470594	-1.19155796715166	0.63593296927078
C	-1.96904293913850	3.96080515017405	3.48319740539149
N	-2.28591768962621	2.62821669532906	2.90412698469317
C	-1.26075487420404	1.61793275560318	3.34980101561858
C	-2.28164685418145	2.69362896971331	1.40242293971097

C	-3.63541155239137	2.14150664933595	3.34614172331062
H	-1.96354038984070	3.88310714272776	4.57808096313274
H	-2.51881592833097	1.66932760747594	1.06347064918445
H	-4.39087814815163	2.88379053328358	3.05389550235934
H	-0.28070737145515	1.93801241429029	2.98044628663385
H	-1.28886894363866	3.02143710153201	1.07525018948370
H	-3.04592563407810	3.41654336683304	1.08534943118171
H	-1.25532174405008	1.55485154876993	4.44461340010583
H	-1.55867891103989	0.66325069518722	2.89898398671185
H	-3.62107183074023	2.02259267783383	4.43722885340343
H	-3.78253684894992	1.17476063828108	2.82847974923064
H	-0.97727147439906	4.27000263753423	3.12807043349018
H	-2.72492882261711	4.68926885900603	3.15993505505554
F	-2.97912635007204	-0.09888077497311	1.65378052830247

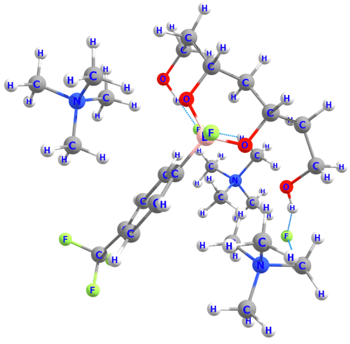

Coordinates from ORCA-job orca

C	1.11247322326080	-2.09503145908692	2.63295226748210
C	2.50219856227935	-2.26615521870479	2.72916771139237

C	3.40159313202722	-1.27871216328352	2.30690488838444
C	2.90518957636718	-0.08729027716972	1.76397429229783
C	1.51744008598537	0.10646723781381	1.65588977173716
C	0.63529551958675	-0.88501568855898	2.08490010702333
C	3.84475275364631	0.93041867915447	1.19328814255676
F	4.02228363807524	0.74405288705720	-0.14166888226169
B	0.03727699649165	-3.23170181099905	3.09473160020335
O	-0.68338802648488	-2.71991244918884	4.26159904090863
C	-1.95924076276231	-3.26050277637560	4.52754470642721
C	-2.73332599525221	-2.49060548200363	5.62195915795174
C	-1.92685329740188	-1.73154121619764	6.67033021703364
O	-1.35813633972002	-0.60219663231859	6.08806356716715
F	3.39614503673827	2.19078944605707	1.34106314583439
F	5.07072753888653	0.87467077130580	1.74886489452719
F	0.72697445413403	-4.44687919280924	3.43987314230680
O	-0.81198406315243	-3.47789869771334	1.91014567625730
C	-2.10666801168535	-4.00981184246603	2.11980886221828
C	-2.79137159566310	-3.24764094408678	3.24606771271416
C	-0.28189119425331	-2.31612625964805	-0.97716117584859
N	0.93511021051720	-3.16317837421049	-1.27601218041770
C	2.15162643917030	-2.52486608641610	-0.68387103900407
C	1.11239372840151	-3.30250664540896	-2.74787785064960
C	0.72412845268674	-4.50913403535209	-0.63968784797996

H	-0.49315674079639	-2.36003683765761	0.09726371495063
H	1.98363305238341	-3.93915296219834	-2.95163165450655
H	-0.10775369528731	-5.00370007878570	-1.15657228186102
H	2.27091073865146	-1.51483732089938	-1.09270246155166
H	2.88382506511000	-3.21131856900811	3.12769092830392
H	4.48127406952564	-1.43181165612431	2.38040198513736
H	1.13275386131755	1.03848237113713	1.23369348782504
H	-0.44803394466434	-0.72616309671082	1.99026524433098
H	-2.00609974693557	-5.07449868803189	2.42719821213086
H	-1.83485320580594	-4.31152335505739	4.87174899793626
H	-2.88504015277843	-2.19271540969640	2.93960843920278
H	-3.79853475433105	-3.65955927959593	3.43529228925610
H	-3.40242186303540	-3.21101719713265	6.12526637369037
H	-3.38388035065644	-1.74507302179417	5.13671436054498
H	-2.60108146417890	-1.46360519998992	7.51122730425716
H	-1.15475039914199	-2.41063609654363	7.10650680924215
H	-1.20012375242777	0.24480825151832	6.65013590437331
H	1.26706714919043	-2.30681634337730	-3.18302962702148
H	0.20943386599358	-3.75492229980372	-3.17591242628227
H	2.01842978374399	-2.46845492086372	0.39910359871756
H	3.02844770014010	-3.13943604529483	-0.92543428196383
H	0.44294202221894	-4.35135349856436	0.41561663548296
H	1.64252537884222	-5.10110385368322	-0.74557436873887

H	-0.09137225044929	-1.28954966342356	-1.31048821257959
H	-1.13824838254477	-2.73381311978869	-1.51229882440611
C	-2.93166368597088	-3.99593914826768	0.82201456100427
H	-3.74414619288502	-4.73724594049042	0.94183809516482
H	-2.29646566604355	-4.37860044047565	0.00261184514757
H	-4.24222033374230	-2.92444374775995	-0.48598048293474
C	-3.60192295258571	-2.67735799141434	0.38800432694152
H	-4.30090147743159	-2.35862737408055	1.18616675352685
O	-2.74086191935802	-1.63766155963684	0.03383399075378
H	-2.61610758855323	-1.00418837023998	0.82220115751880
C	-2.91897272554380	2.76393445759417	2.71685714633416
N	-2.46357882428475	2.25282240949668	4.04502499432467
C	-2.46377350507452	3.30157947809120	5.11025376890208
C	-1.06290306432538	1.72161996623474	3.90898838907873
C	-3.36892483547822	1.11543950833387	4.43789271573822
H	-3.95826008856257	3.10934034452386	2.80475914211559
H	-0.73548091256521	1.46816682386263	4.92256618195589
H	-3.33267163996440	0.40124001550701	3.59900947617599
H	-1.86380991819538	4.15336243692577	4.76032916468489
H	-0.43929671926757	2.52160541480815	3.48484151876430
H	-1.12334490093781	0.85873065581460	3.23493285924854
H	-3.49688102981394	3.62712972226783	5.29389627501673
H	-1.99592558145114	2.85810222298808	6.00920351133840

H	-4.37556323470886	1.52370052821998	4.60171241304198
H	-2.95478164667647	0.65428274316526	5.33977326126459
H	-2.27263810544254	3.59978759952895	2.41604616586556
H	-2.83445789850763	1.90978565279987	2.02306653577930
F	-2.40127617255088	-0.09699491842277	1.96376215345963
C	2.00138283373952	-2.21774732038411	6.13176062664357
N	2.00394166298477	-0.74761814167371	6.43934095214364
C	1.41784215311042	-0.00955010301978	5.26420949389870
C	3.39795359704067	-0.26734426294871	6.65381474716376
C	1.19119073691311	-0.49025967932350	7.68733191888263
H	0.99566546852260	-2.50339321633759	5.78521328908682
H	3.36474788588256	0.79625853415239	6.92295262833297
H	1.84769807935619	-0.62924654295893	8.55660557049959
H	2.09174457172575	-0.13997910251208	4.41281113493814
H	3.96706843274493	-0.39767212240987	5.72463168518028
H	3.86216263269553	-0.84374691771754	7.46477492461706
H	0.42564129771839	-0.43509632816820	5.07119306748494
H	1.31837534041391	1.04256158868613	5.55044527454375
H	0.38008760888925	-1.22143319644355	7.71178639337999
H	0.72780479259282	0.51277718519389	7.63307479454696
H	2.71321733902007	-2.40916501418129	5.32232984497224
H	2.29404918853994	-2.76547835863025	7.03724246079664
F	-0.72603577293176	1.56679045528244	6.96724432094293

8 References

(1) Neese, F. Software Update: The ORCA Program System, Version 4.0. *Wiley Interdiscip. Rev. Comput. Mol. Sci.* **2018**, *8* (1), 4–9.

(2) Becke, A. D. Density-Functional Thermochemistry. III. The Role of Exact Exchange. *J. Chem. Phys.* **1993**, *98* (7), 5648–5652.

(3) Weigend, F.; Ahlrichs, R. Balanced Basis Sets of Split Valence, Triple Zeta Valence and Quadruple Zeta Valence Quality for H to Rn: Design and Assessment of Accuracy. *Phys. Chem. Chem. Phys.* **2005**, *7* (18), 3297–3305.

(4) Grimme, S.; Antony, J.; Ehrlich, S.; Krieg, H. A Consistent and Accurate Ab Initio Parametrization of Density Functional Dispersion Correction (DFT-D) for the 94 Elements H-Pu. *J. Chem. Phys.* **2010**, *132* (15), 154104.

(5) Grimme, S.; Ehrlich, S.; Goerigk, L. Effect of the Damping Function in Dispersion Corrected Density Functional Theory. *J. Comput. Chem.* **2011**, *32* (7), 1456–1465.

(6) Rappoport, D.; Furche, F. Property-Optimized Gaussian Basis Sets for Molecular Response Calculations. *J. Chem. Phys.* **2010**, *133* (13), 134105.

(7) Weigend, F. Accurate Coulomb-Fitting Basis Sets for H to Rn. *Phys. Chem. Chem. Phys.* **2006**, *8* (9), 1057–1065.

(8) Neese, F.; Wennmohs, F.; Hansen, A.; Becker, U. Efficient, Approximate and Parallel Hartree-Fock and Hybrid DFT Calculations. A “chain-of-Spheres” Algorithm for the Hartree-Fock Exchange. *Chem. Phys.* **2009**, *356* (1–3), 98–109.

(9) Dutta, A. K.; Neese, F.; Izsák, R. Speeding up Equation of Motion Coupled Cluster Theory with the Chain of Spheres Approximation. *J. Chem. Phys.* **2016**, *144* (3), 034102.

(10) Yanai, T.; Tew, D. P.; Handy, N. C. A New Hybrid Exchange-Correlation Functional Using the Coulomb-Attenuating Method (CAM-B3LYP). *Chem. Phys. Lett.* **2004**, *393* (1–3), 51–57.

(11) Borges, I.; Uhl, E.; Modesto-Costa, L.; Aquino, A. J. A.; Lischka, H. Insight into the Excited State Electronic and Structural Properties of the Organic Photovoltaic Donor Polymer Poly(Thieno[3,4-b]Thiophene Benzodithiophene) by Means of Ab Initio and Density Functional Theory. *J. Phys. Chem. C* **2016**, *120* (38), 21818–21826.

(12) Kołaski, M.; Arunkumar, C. R.; Kim, K. S. Aromatic Excimers: Ab Initio and TD-DFT Study. *J. Chem. Theory Comput.* **2013**, *9* (1), 847–856.

(13) Hudlicky, M. Chemical Shifts of Fluorine in Hydrogen Fluoride and Fluoride Ion. *J. Fluor. Chem.* 1985, *28*, 461-472.